





Intrinsic suppression of type I interferon production underlies the therapeutic efficacy of IL-15-producing natural killer cells in B-cell acute lymphoblastic leukemia

Anil Kumar ¹, Adeleh Taghi Khani,¹ Caroline Duault ², Soraya Aramburo,¹ Ashly Sanchez Ortiz,¹ Sung June Lee,¹ Anthony Chan ¹, Tinisha McDonald,³ Min Huang,⁴ Norman J. Lacayo,⁴ Kathleen M. Sakamoto,⁴ Jianhua Yu,⁵ Christian Hertz,⁶ Martin Carroll,⁷ Sarah K. Tasian ⁸, Lucy Ghoda,⁹ Guido Marcucci,^{3,5,9} Zhaohui Gu,¹ Steven T. Rosen,⁵ Saro Armenian,¹⁰ Shai Izraeli,^{1,11} Chun-Wei Chen,¹ Michael A. Caligiuri,⁵ Stephen J. Forman,⁵ Holden T. Maecker,² Srividya Swaminathan ^{1,10}

To cite: Kumar A, Taghi Khani A, Duault C, *et al*. Intrinsic suppression of type I interferon production underlies the therapeutic efficacy of IL-15-producing natural killer cells in B-cell acute lymphoblastic leukemia. *Journal for ImmunoTherapy of Cancer* 2023;11:e006649. doi:10.1136/jitc-2022-006649

► Additional supplemental material is published online only. To view, please visit the journal online (<http://dx.doi.org/10.1136/jitc-2022-006649>).

Accepted 03 May 2023



© Author(s) (or their employer(s)) 2023. Re-use permitted under CC BY-NC. No commercial re-use. See rights and permissions. Published by BMJ.

For numbered affiliations see end of article.

Correspondence to

Dr Srividya Swaminathan; sswaminathan@coh.org

ABSTRACT

Background Type I interferons (IFN-I)s, secreted by hematopoietic cells, drive immune surveillance of solid tumors. However, the mechanisms of suppression of IFN-I-driven immune responses in hematopoietic malignancies including B-cell acute lymphoblastic leukemia (B-ALL) are unknown.

Methods Using high-dimensional cytometry, we delineate the defects in IFN-I production and IFN-I-driven immune responses in high-grade primary human and mouse B-ALLs. We develop natural killer (NK) cells as therapies to counter the intrinsic suppression of IFN-I production in B-ALL.

Results We find that high expression of IFN-I signaling genes predicts favorable clinical outcome in patients with B-ALL, underscoring the importance of the IFN-I pathway in this malignancy. We show that human and mouse B-ALL microenvironments harbor an intrinsic defect in paracrine (plasmacytoid dendritic cell) and/or autocrine (B-cell) IFN-I production and IFN-I-driven immune responses. Reduced IFN-I production is sufficient for suppressing the immune system and promoting leukemia development in mice prone to MYC-driven B-ALL. Among anti-leukemia immune subsets, suppression of IFN-I production most markedly lowers the transcription of IL-15 and reduces NK-cell number and effector maturation in B-ALL microenvironments. Adoptive transfer of healthy NK cells significantly prolongs survival of overt ALL-bearing transgenic mice. Administration of IFN-I to B-ALL-prone mice reduces leukemia progression and increases the frequencies of total NK and NK-cell effectors in circulation. Ex vivo treatment of malignant and non-malignant immune cells in primary mouse B-ALL microenvironments with IFN-I fully restores proximal IFN-I signaling and partially restores IL-15 production. In B-ALL patients, the suppression of IL-15 is the most severe in difficult-to-treat subtypes with MYC overexpression. MYC overexpression promotes sensitivity of B-ALL to NK cell-mediated killing.

WHAT IS ALREADY KNOWN ON THIS TOPIC

⇒ NK cells engineered to secrete IL-15 were found to be efficacious in clinical trials of patients with non-acute lymphoblastic leukemia (ALL) hematopoietic malignancies. However, their therapeutic potential in patients with B-ALL and the mechanisms underlying their efficacy in ALL were unknown.

WHAT THIS STUDY ADDS

⇒ We find that intrinsic blockade in type I interferon (IFN-I) production suppresses IL-15 expression and IL-15-induced NK surveillance in high-grade B-ALLs that overexpress the c-MYC oncoprotein. Importantly, MYC overexpression makes B-ALL cells sensitive to eradication by IL-15-producing NK cells.

HOW THIS STUDY MIGHT AFFECT RESEARCH, PRACTICE OR POLICY

⇒ Our study rationalizes the extensive preclinical and clinical development of IL-15-secreting NK cell-based therapies for poor prognosis B-ALL subtypes that overexpress the difficult-to-drug MYC oncoprotein.

To counter the suppressed IFN-I-induced IL-15 production in MYC^{high} human B-ALL, we CRISPRa-engineered a novel human NK-cell line that secretes IL-15. CRISPRa IL-15-secreting human NK cells kill high-grade human B-ALL in vitro and block leukemia progression in vivo more effectively than NK cells that do not produce IL-15.

Conclusion We find that restoration of the intrinsically suppressed IFN-I production in B-ALL underlies the therapeutic efficacy of IL-15-producing NK cells and that such NK cells represent an attractive therapeutic solution for the problem of drugging MYC in high-grade B-ALL.

INTRODUCTION

B-cell acute lymphoblastic leukemia (B-ALL) is an aggressive form of childhood and adult lymphoid malignancy.¹ With recent advances in targeted and cellular immunotherapies,^{2,3} 90% of childhood B-ALL is curable. However, only 30%–40% of adults with B-ALL are cured.¹ Specific pediatric and adult B-ALL subgroups including those with *KMT2A* or *MYC/BCL2* rearrangements and hypodiploidy are challenging to treat.⁴ First-line chemotherapy, although effective in killing B-ALL cells, is toxic and worsens immunosuppression in many patients.⁵ Therefore, targeted strategies that concurrently kill leukemia cells while reversing immunosuppression in B-ALL patients must be developed. To this end, we must delineate the mechanisms dampening the anti-leukemia host immune responses in B-ALL.

Among immunosuppression pathways, we focus on the inactivation of IFN-I signaling and responses. The IFN-I pathway is one of the first lines of anticancer immune defenses, as exemplified in solid tumor models where genetic ablation of IFN-I receptor drives immunoediting and tumorigenesis.⁶ However, the biology and importance of IFN-I pathway in hematopoietic cancers including B-ALL is less understood.

Expression of IFN-I-stimulated genes (ISGs) was found to be differentially regulated across specific B-ALL subgroups.⁷ We and others found that targeted inactivation of driver oncogenes including *MYC* and treatment with epigenetic therapies induce autocrine production of IFN-Is from malignant B cells in vitro.^{8,9} However, these studies did not determine if expression of IFN-I signaling and ISGs are predictive of clinical outcome in B-ALL patients, the extent to which autocrine (B-cell) and paracrine (non-B-cell) IFN-I production, signaling, and/or responses are suppressed in B-ALL compared with their healthy counterparts, and whether such suppression could be reversed with IFN-I treatment.

Surprisingly, IFN-Is have not been used as single agent therapies for acute leukemia. IFN-Is were combined with bone marrow (BM) transplantation to prolong remission in patients with B-ALL.¹⁰ Recently, IFN-Is were found to enhance relapse-free survival (RFS) in acute myeloid leukemia (AML) patients who underwent allogeneic BM transplantation.¹¹ We hypothesized that the poor efficacy of IFN-Is as a single agent therapy for acute leukemia results from reduction in IFN-I response from anti-leukemia immune subsets such as natural killer (NK) cells.¹² We further postulated that the absence of IFN-I responding anti-leukemia immune cells in B-ALL is initiated by an intrinsic block in IFN-I production and/or response during primary leukemogenesis.

Here, we show that high expression of IFN-I response genes predicts favorable clinical prognosis in B-ALL patients. Using diagnosis samples from B-ALL patients and an aggressive *MYC*-driven B-ALL-prone transgenic mouse model with germline ablation of IFN-I signaling, we determine the mechanism(s) of suppression of IFN-I signaling during primary leukemogenesis and the consequences of

this suppression on anti-leukemia immune surveillance. We observe that B-ALLs exhibit suppressed production of autocrine (B cell-derived) and paracrine (plasmacytoid dendritic cell (pDCs)-derived) IFN-Is. This intrinsic suppression in IFN-I production is sufficient for overt leukemogenesis. Among anti-leukemic immune subsets, NK cells are the most sensitive to suppression of IFN-I production in B-ALL due to the reduced production of the IFN-I-stimulated cytokine, interleukin (IL)-15, that is, produced by conventional DCs (cDCs) and is indispensable for NK-cell homeostasis.^{13,14} Suppression of IL-15 was more severe in B-ALL patients who expressed high levels of *MYC*.¹⁵

Translating our observations, we modified our novel CRISPRa-based NK-cell platforms¹⁶ to engineer soluble IL-15-producing NK cells that kill B-lymphoblasts and can potentially persist in B-ALL microenvironments devoid of IL-15 and IFN-Is. We find IL-15-producing allogeneic NK cells to be an effective approach to reverse the detrimental effects of natural suppression of IFN-I production in certain high-risk B-ALLs.

METHODS

Patient samples

Deidentified diagnosis B-ALL patient BM mononuclear cells (BMMCs) and peripheral blood mononuclear cells (PBMCs) were obtained from the City of Hope Hematopoietic Tissue Biorepository and University of Pennsylvania Stem Cell and Xenograft Core after informed consent per Institutional Review Board policies. Age-matched healthy BMMCs were purchased from AllCells (Alameda, California, USA) and Stem Cell Technologies (Vancouver, Canada). Age-matched healthy PBMCs were isolated from buffy coats procured from the City of Hope Michael Amini Transfusion Medicine Center. Patient samples analyzed include a new cohort in online supplemental table S1 and a cohort reported in our recent publication.¹²

Cell lines and cell culture

Mycoplasma-negative human cell lines (NK-92, K562, SEM, KOPN8, P493-6, VAL, and MHH-CALL4) were obtained from American Type Culture Collection or Deutsche Sammlung von Mikroorganismen und Zellkulturen and cultured in Roswell Park Memorial Institute (RPMI)-1640 with 10% fetal bovine serum (FBS), 100 U/mL penicillin, and 100 µg/mL streptomycin (complete RPMI, Invitrogen/Life technologies). NK-92 cells were cultured in the presence of recombinant human IL-2 (100 U/mL, R & D Systems). In P493-6 cells, *MYC* expression is tetracycline-regulated¹⁷ and *MYC* was inactivated by treating cells with 0.2 µg/mL doxycycline for 24 hours.

Mouse strains

To generate *Eμ-Myc* (hemizygous)/*IFNARI*^{-/-} mice, *Eμ-Myc* males were crossed with *IFNARI*^{-/-} females, and F1 progeny *Eμ-Myc*/ *IFNARI*^{+/-} males were backcrossed

with *IFNAR1*^{-/-} females. Transnetyx conducted genotyping. *Eμ-Myc* and *Eμ-Myc/IFNAR1*^{-/-} mice were monitored for visible symptoms of B-ALL including hunched posture, shortness of breath, visible lumps, and ruffled fur. Spleen and BM cells were harvested from euthanized B-ALL mice and cryopreserved in FBS containing 10% dimethyl sulfoxide and stored in liquid nitrogen.

Cytometry

For flow cytometry surface staining, cells were thawed in complete RPMI and stained with fluorochrome-tagged surface antibodies and Ghost Dye UV 450 for 30 min on ice, followed by acquisition on a BD FACSymphony cytometer. For IFN α 2b detection, cells were rested in complete RPMI for 3 hours at 37°C and treated with 3 μ M class C CpG oligodeoxynucleotides (CpG ODN) for 2 hours at 37°C. After adding eBioscience Protein Transport Inhibitor Cocktail (1X) for 3 hours, cells were incubated overnight in 100 μ L/mL of 20 mM EDTA at 4°C. The next day, cells were washed, surface stained, fixed and permeabilized using BD fix/perm buffer kit and incubated with IFN α 2b antibody for 1 hour at room temperature (RT). To stain pSTAT1, cells were incubated at 37°C for 30 min, stimulated with IFN β for 15 min, and fixed with 1% paraformaldehyde (Biolegend). Cells were permeabilized with 0.5X Perm Buffer IV (BD Biosciences), washed, and stained with anti-pSTAT1 antibody for 1 hour at RT. Data were acquired on BD FACSymphony cytometer and analyzed using FlowJo V.10.7.1.

Mass cytometry was carried out as before.^{12, 18} Thawed samples, split into ‘unstimulated’ and ‘stimulated’ conditions, were rested overnight. ‘Stimulated’ cells were incubated with Phorbol 12-myristate 13-acetate (PMA)/Ionomycin for 4 hours. During incubation, brefeldin A and monensin (MilliporeSigma) were added in both conditions. After incubation, 2 mM EDTA was added for 15 min. Washed cells were stained for surface proteins and intracellular cytokines, followed by DNA staining with Cell-ID Intercalator-Ir (Standard BioTools). Data were normalized using MATLAB (<https://github.com/nolanlab/bead-normalization/releases>) and analyzed using Cytobank (Beckman Coulter,¹⁹). Online supplemental tables S2 and S3 contain cytometry antibodies.

Adoptive transfer of NK cells into B-ALL-bearing mice

Syngeneic NK cells were isolated from healthy *UBC-GFP* mice using Miltenyi Biotec mouse NK-cell isolation kit per manufacturer’s instructions. On onset of visible signs of B-ALL, 7 \times 10⁵ NK cells or PBS was intravenously injected into *Eμ-Myc* mice and leukemia-free survival was measured.

NK-cell proliferation and cytotoxicity

CRISPRa-engineered NK-92 cells were generated as described previously.¹⁶ To measure NK-cell proliferation, control-single guide RNA and IL-15-single guide RNA (sgRNA) transduced NK-92 cells were cultured in triplicates without (100,000 cells/well) or with 100 IU/mL IL-2 (50,000 cells/well) in complete RPMI-1640 media in a flat

bottom 96-well-plate for 96 hours. After excluding dead cells using trypan blue, live cells were counted using a hemocytometer.

To measure NK cytotoxicity, targets were labeled with 2.5 μ M carboxyfluorescein succinimidyl ester-violet dye and cocultured with either CRISPRa control-sgRNA or IL-15-sgRNA transduced NK-92 cells at an effector-to-target ratio of 10:1 in complete RPMI. After 5 hours, cells were stained with 7-aminoactinomycin D (7-AAD). Cytotoxicity was measured on BD FACSymphony flow cytometer and analyzed using FlowJo V.10.7.1. Specific cytotoxicity = ((7-AAD⁺target cell frequency in coculture with effector cells–7-AAD⁺ target cell frequency alone)/(100–7-AAD⁺ target cell frequency alone)) \times 100.

ELISA

1 \times 10⁶ control-sgRNA and IL-15-sgRNA transduced NK-92 cells were stimulated with PMA (5 ng/mL) and ionomycin (0.5 μ g/mL) for 24 hours at 37°C. IL-15 level was measured in culture supernatant using high-sensitivity human IL-15 ELISA kit (#41702) from PBL Assay Science as per manufacturer’s instructions.

Ex vivo treatment of mouse splenocytes with IFN-Is

2 \times 10⁶/mL splenocytes were treated for 8 hours with 10,000 IU/mL IFN β (R&D Systems) in complete RPMI, washed, followed by downstream analysis.

Administration of IFN β to B-ALL-prone mice

Tail vein peripheral blood of *Eμ-MYC* B-ALL-prone mice aged ~7–20 weeks was drawn to measure frequencies of immune cells before administration of IFN β . Mice were then treated intraperitoneally with 50,000 IU/100 μ L of IFN β or 100 μ L PBS for 9 days. On day 9, mice were euthanized and circulating immune cells were collected by cardiac puncture for flow cytometry.

Lentivirus production and transduction

Firefly luciferase lentivirus was produced from Lenti-X 293T human embryonic kidney cells (Takara Bio) by transfecting with plasmids containing luciferase (pLenti CMV Puro LUC, w168-1; Addgene), packaging (psPAX2; Addgene), and envelope (pMD.2G; Addgene) genes using lipofectamine 2000 (Invitrogen) in serum free media for 3 hours. Cells were supplemented with addition of high glucose complete Dulbecco’s Modified Eagle Medium (DMEM, Invitrogen) media containing 100 IU/mL penicillin, 100 μ g/mL streptomycin, 10% FBS, 25 mM HEPES (4-(2-hydroxyethyl)-1-piperazineethanesulfonic acid), pH 7.2, 1 mM sodium pyruvate and 0.1 mM nonessential amino acids. Next day, media was removed, and cells were incubated in complete DMEM containing 20 mM sodium butyrate (Alfa Aesar) for 5 hours. After 5 hours of incubation, media was changed back to complete DMEM without sodium butyrate. Next day, viral culture supernatant was collected, passed through a 0.45 μ m filter, and concentrated with Lenti-X Concentrator (Takara Bio) per manufacturer’s instructions. Concentrated lentivirus was resuspended in 1 mL complete RPMI media. A 500 μ L of concentrated virus was mixed with 500 μ L of complete RPMI

media containing 2×10^6 P493-6 cells and 8 $\mu\text{g/mL}$ polybrene (Millipore Sigma). After 48 hours, cells were washed, cultivated, and selected in puromycin (1 $\mu\text{g/mL}$)-containing complete RPMI.

B-ALL cell line-derived xenograft mouse model to test the efficacy of CRISPRa-IL-15-producing human NK cells

1×10^6 P493-6 cells were luciferase-labeled and injected intravenously into 4–6 weeks *NOD-SCIDIL-2R $\gamma^{-/-}$* (NSG) mice. Engraftment of P493-6 cells was confirmed by bioluminescence imaging (BLI) using Lago-X (spectral instruments imaging). D-luciferin monosodium salt dissolved in PBS was injected intraperitoneally at 2.5 mg/mouse 12 min before BLI. Mice were kept under general anesthesia (3%–5% isoflurane) during BLI. After verifying B-ALL engraftment on day 9, mice were intravenously injected with either CRISPRa control or IL-15-producing NK-92 cells (7×10^6 NK cells per mouse). BLI was performed twice a week to measure disease progression.

Immunoblotting

Cells were lysed in RIPA buffer (Sigma) supplemented with 1% protease inhibitor ‘cocktail’ (Pierce). Proteins were then separated by electrophoresis through 4%–20% TGX gradient gels (BioRad) and were transferred to polyvinylidene fluoride membranes (Immobilion; Millipore). For the detection of human proteins by immunoblot analysis, we used primary antibodies listed in online supplemental table S5 and western enhanced chemiluminescence (BioRad). Blots were developed in ChemiDoc MP imaging system (BioRad).

Quantitative real-time PCR (qPCR)

RNA was extracted using NucleoSpin RNA Plus kit * (MACHERY-NAGEL) per manufacturer’s instructions. cDNA was synthesized using SuperScript IV Reverse Transcriptase (Invitrogen). qPCR was conducted using Power SYBR Green PCR master mix (ThermoFisher Scientific) and QuantStudio V.7 flex real-time PCR system (Applied Biosystems). Online supplemental table S4 lists qPCR primers.

Statistics

Statistical tests are two tailed. Exact p values are provided if significant ($p < 0.05$) or trending toward significance ($0.05 < p < 0.1$). Mann-Whitney U test was used for pairwise comparisons between mouse cohorts. Kaplan-Meier survival p values were calculated using log-rank test. Sample size was calculated using ‘cpower’ function in R package. Each biological qPCR sample was run in three technical replicates. Cell-line experiments were repeated three times for reproducibility.

RESULTS

Intrinsic suppression of IFN-I production and response in B-ALL predicts poor clinical outcome

We hypothesized that expression of IFN-I signaling and response genes, being a measure of anti-leukemia immune surveillance, can predict clinical outcome in patients with B-ALL. To determine the importance of

IFN-I signaling in B-ALL, we compared RFS probabilities of 207 children with high-risk B-ALL from the Children’s Oncology Group P9906 clinical trial^{20 21} divided into two groups based on their median expression of IFN-I signaling and response genes IFNAR1, IFNAR2, STAT1, MX1, and OAS1 at diagnosis. Patients with higher than median expression of all IFN-I signaling/response genes ($n=15$) had significantly longer RFS probabilities as compared with their IFN-I response^{low} counterparts ($n=14$) (figure 1A). Patients with high IFN-I response were ~3 times less likely (13%) to have white blood cell (WBC) counts of $\geq 100,000/\mu\text{L}$ that often correlate with poor clinical prognosis, compared with their low IFN-I response counterparts (43%) (figure 1B). Compared with better prognosis IFN-I response^{high} counterparts, poor prognosis IFN-I response^{low} B-ALL patients had reduced expressions of interferon regulatory factor 7 (IRF7), the gene indispensable for IFN-I production²² and CD123, a marker highly expressed by IFN-I producing immune cells^{23 24} (figure 1C). Consistent with the above, patients with high concomitant expression of IFN-I response genes, IRF7, and CD123 ($n=13$) fared better and were more likely to have WBC counts of $< 100,000/\mu\text{L}$ at diagnosis compared with patients with low expression of IFN-I signaling genes, IRF-7, and CD123 ($n=9$) (online supplemental figure S1).

The above findings suggested that B-ALL may be associated with an intrinsic defect in IFN-I production and consequently, in IFN-I mediated responses. Therefore, we compared the proportion of IFN-I (IFN $\alpha 2b$)-producing cells in ODN-stimulated tissue-matched and age-matched samples from healthy donors and B-ALL patients (online supplemental table S1) using high-dimensional flow cytometry (online supplemental figure S2A,B). We observed significant reductions in total IFN-I⁺ cells in BMMCs and PBMCs of B-ALL patients (figure 1D,E). Hence, the ALL microenvironment has suppressed IFN-I production.

We determined which IFN-I-producing immune subset(s) are suppressed in B-ALL. First, we measured IFN-I-producing cells in B-ALL PBMC samples, all of which had CD19⁺ leukemia, allowing distinction of leukemic and anti-leukemic immune fractions. Frequencies of IFN $\alpha 2b$ ⁺ and total pDCs, the ‘professional’ and highest IFN-I producer, were reduced within the non-leukemic immune fraction in stimulated B-ALL compared with healthy PBMC (figure 1F,G). Reduction in pDCs was compensated by an increase in the CD123^{low}CD11c⁺ fraction (figure 1G). Residual pDCs in B-ALL patients expressed increased CXCR4 (figure 1H), a marker that correlates inversely with pDC’s IFN-I production potential.²⁵ Next, we measured frequencies of total pDCs and IFN $\alpha 2b$ ⁺ within non-leukemic fraction only in CD19⁺ BM B-ALLs and found it to be significantly reduced compared with healthy donors (online supplemental figure S3A,B). Cytometry was not sensitive to detect IFN-I in stimulated B cells. We infer that the B-ALL microenvironment harbors an intrinsic defect in IFN-I production.

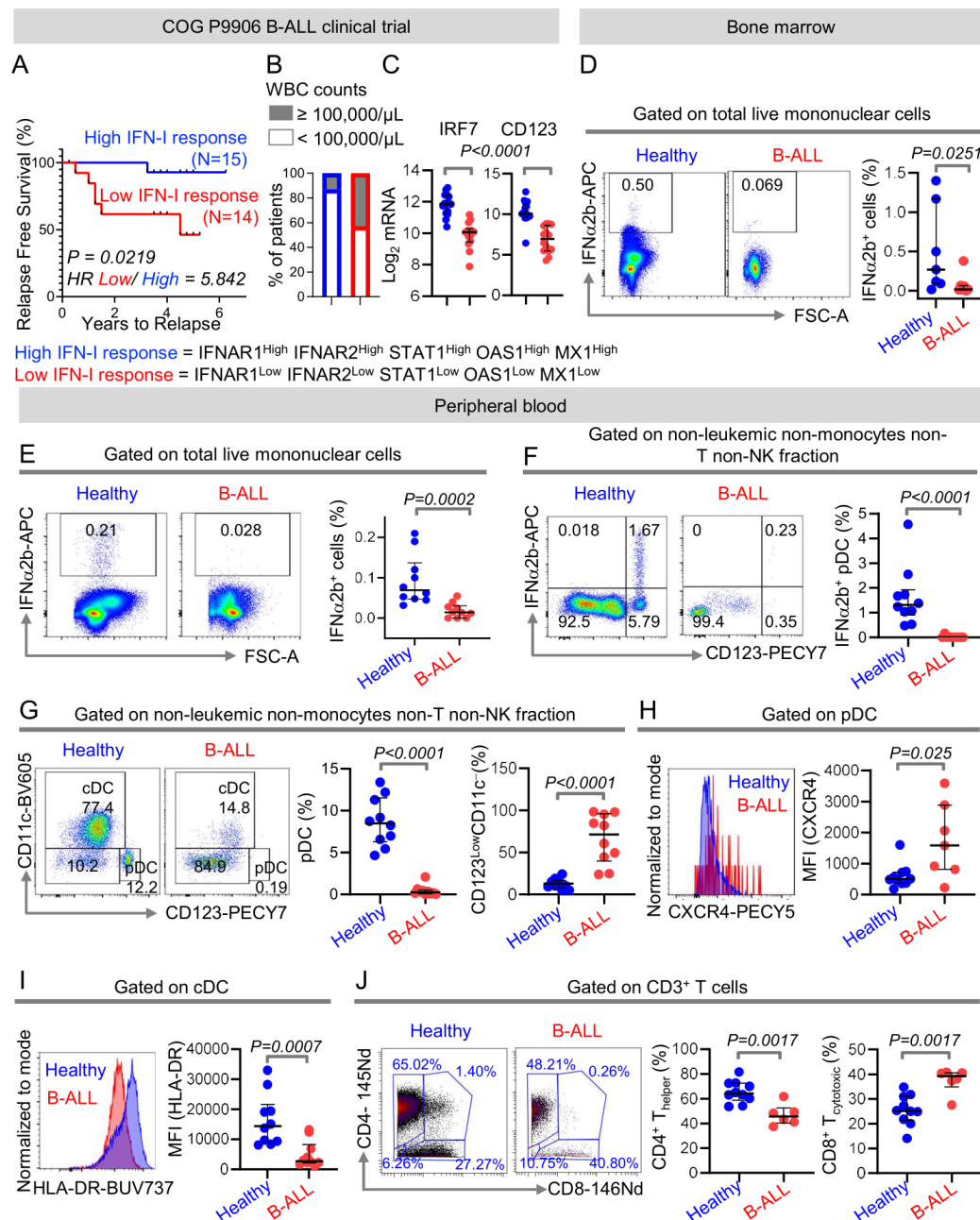


Figure 1 Intrinsic suppression of IFN-I production and response in B-ALL predicts poor clinical outcome. (A) Comparison of relapse-free survival probabilities of COG P9906 B-ALL patients separated into two groups that is, IFNAR1^{High}IFNAR2^{High}STAT1^{High}OAS1^{High}MX1^{High} ('High IFN-I Response', n=15) and IFNAR1^{Low}IFNAR2^{Low}STAT1^{Low}OAS1^{Low}MX1^{Low} ('Low IFN-I Response' n=14) based on the median transcript expression of these genes. (B) Stacked bar charts comparing the proportions of COG P9906 B-ALL patients with WBC counts $\geq 100,000/\mu\text{L}$ or WBC counts $< 100,000/\mu\text{L}$ within the 'High IFN-I Response' and 'Low IFN-I Response' cohorts. (C) Comparison of IRF7 and CD123 transcript levels within the 'High IFN-I Response' and 'Low IFN-I Response' cohorts. (D-F) Comparison of IFN $\alpha 2b^+$ cells in class C CpG ODN-stimulated total BMMCs (D), total PBMCs (E), and within the HLA-DR⁺ non-B, non-monocytes, non-T, and non-NK immune cell fraction of PBMCs (F) between B-ALL patients (n=7 BMMC, n=10 PMBC) and healthy donors (n=7 BMMC, n=10 PMBC) by flow cytometry. (G) Comparison of peripheral blood pDC frequencies within the HLA-DR⁺ non-B, non-monocytes, non-T, and non-NK immune cell fractions between B-ALL patients (n=10) and healthy donors (n=10) by flow cytometry. (H) Median fluorescence intensity (MFI) of CXCR4 expression on peripheral blood pDCs of B-ALL patients (n=7) and healthy donors (n=10) by flow cytometry. (I) MFI of HLA-DR expression on peripheral blood cDC of B-ALL patients (n=10) and healthy donors (n=10). (J) Analysis of frequencies of CD4⁺ and CD8⁺ T cells within non-leukemic pan T-cell fraction of B-ALL patients (n=6) and healthy donors (n=10) using mass cytometry. For all flow cytometry experiments, one representative histogram or dot plot from each group is shown. Survival was calculated by Kaplan-Meier method and p value calculated by log-rank test. All other comparisons between any two groups were conducted using Mann-Whitney U test. Exact p values are provided whenever significant. B-ALL, B-cell acute lymphoblastic leukemia; BMMC, bone marrow mononuclear cell; cDC, conventional dendritic cell; PMBC, peripheral blood mononuclear cell; pDC, plasmacytoid DC; WBC, white blood cell.

Our recent findings of impaired NK-cell maturation and cytotoxicity in B-ALL patients,¹² provide a biological foundation for our hypothesis that IFN-I-driven immune responses are suppressed in B-ALL. Because IFN-Is drive immune homeostasis, we predicted that reduced IFN-I production in B-ALL may suppress immune surveillance beyond NK cells. Therefore, we analyzed phenotypes of non-NK immune subsets as readouts of dampened IFN-I production in B-ALL by flow and mass cytometry (online supplemental figure S4). We found reduced expression of major histocompatibility class II (MHCII), a downstream target of IFN-I response,²⁶ in antigen-presenting DCs (figure 1I) and B cells (online supplemental figure S5) of B-ALL patients. Significantly reduced frequencies of CD4⁺ T helper cells within the CD3⁺ T-cell fraction (figure 1J) lead us to speculate that suppressed IFN-I production in B-ALL may impair antigen presentation (MHCII) and subsequent T helper-cell multiplication and anti-leukemia immune responses.^{27 28} Overall, IFN-I production is impaired in B-ALL patients and such impairment is associated with suppression of anti-leukemia immune surveillance and poor prognosis.

Intrinsic suppression of IFN-I production is sufficient to drive overt B-cell leukemogenesis

In solid tumor mouse models, germline deletion of the IFN-I receptor, *IFNAR1*, accelerates tumorigenesis.^{6 29} Whether *IFNAR1* deletion accelerates B-cell leukemogenesis and the extent to which intrinsically suppressed IFN-I production in B-ALL (figure 1) impacts this process is unknown. To address this, we generated B-ALL-prone mice lacking both copies of the *IFNAR1* (*IFNAR1*^{-/-}/*Eμ-MYC*). *Eμ-MYC* was chosen because: (1) it models high-risk B-ALL driven by the ‘difficult-to-drug’ MYC oncogene,^{30 31} and (2) we showed MYC transcriptionally represses IFN-I production in malignant B cells in vitro,⁹ suggesting intrinsic suppression of IFN-I production in *Eμ-MYC* mice.

Contrary to observations in solid tumors,⁶ germline deletion of *IFNAR1* did not accelerate B-ALL development (figure 2A). We predicted that unaltered latency to overt leukemogenesis after *IFNAR1* deletion in *Eμ-MYC* mice may be caused by intrinsic suppression of IFN-I production. To test this, after validating the germline ablation of *IFNAR1* in spleen and BM WBCs by quantitative real time PCR (qPCR) (figure 2B, online supplemental figure S6 and S7A), we compared splenic pDC frequencies and counts in healthy, *Eμ-MYC*, and *IFNAR1*^{-/-}/*Eμ-MYC* mice. As predicted, pDCs were reduced to the same extent in B-ALL-bearing mice with or without the *IFNAR1* compared with their healthy counterparts (figure 2C).

We compared expression of IFN-I and ISG transcripts in BM and splenic WBCs of healthy, *Eμ-MYC*, and *IFNAR1*^{-/-}/*Eμ-MYC* mice. Sufficient splenic cells were available to measure IFN-Is and ISGs in the leukemic (B-cell) and non-leukemic (non-B-cell) fractions separately (online supplemental figure S6). For BM, bulk WBCs were used. IFN-I transcript expression was reduced to the same

extent in splenic leukemic fraction and total BM WBCs, in *IFNAR1*^{+/+} and *IFNAR1*^{-/-} B-ALL-bearing mice (figure 2D, online supplemental figure S7B). IFN-I expression in the non-leukemic splenic fraction containing pDCs was unaltered, likely because pDCs form a very small proportion of this fraction and other cells in this fraction do not produce IFN-Is (online supplemental figure S8A). Expression of IFN-I signaling (STAT1), and response genes (MX1, OAS1) was suppressed independently of the *IFNAR1* genotype in splenic leukemic and non-leukemic fractions and BM of B-ALL-bearing mice (figure 2E,F, online supplemental figure S7C and S8B,C).

To determine whether exogenous IFN-Is can rescue ISG suppression in B-ALL, we compared the expressions of STAT1, MX1, and activation/phosphorylation of STAT1 after ex vivo stimulation of primary splenic samples from healthy and B-ALL-bearing *Eμ-MYC* mice. IFN-I stimulation increased expression and activation of IFN-I pathway genes to the same extent (or more) in B-ALL spleens compared with healthy spleens (figure 2G,H). Hence, the natural defect in IFN-I pathway in B-ALL lies in the first step, that is, in IFN-I production and this defect precludes any downstream suppression of IFN-I responses, such as ablation of *IFNAR1*.

Reduced IFN-I production in B-ALL is sufficient to suppress IL-15 and systemically impair NK surveillance

We compared indicators of IFN-I-mediated anti-leukemia immune surveillance in spleen and BM of healthy, *Eμ-MYC* and *IFNAR1*^{-/-} *Eμ-MYC* mice by flow cytometry (online supplemental figure S9). Consistent with the identical suppression of the IFN-I pathway and latency to overt leukemia in *Eμ-MYC* and *IFNAR1*^{-/-} *Eμ-MYC* mice (figure 2), no significant enhancement in suppression of immune subsets was seen after genetic ablation of the *IFNAR1* in *Eμ-MYC* mice. For example, B-ALL-bearing mice with and without *IFNAR1* exhibited similar reduction in numbers of splenic NK1.1⁺NKp46⁺ NK cells, CD3⁺ pan T cells, CD4⁺ Th cells, CD8⁺ Tc cells as compared with normal mice (figure 3A, online supplemental figure S10A). While splenic cDC numbers were unaltered between healthy and B-ALL bearing mice, the frequency of cDCs expressing MHCII was reduced in B-ALL-bearing mice with or without *IFNAR1* (online supplemental figure S10A,B). In BM, only NK cells were highly sensitive to the suppressed IFN-I production and were unaffected by *IFNAR1* deletion. In contrast, T-cell numbers were reduced in BM of B-ALL-bearing mice only on *IFNAR1* ablation (figure 3B, online supplemental figure S11).

Because NK cells are consistently reduced independently of the *IFNAR1* status in two different leukemia microenvironments, we focused on IFN-I-driven NK responses. IFN-Is positively impact NK cell effector maturation both by directly binding to the IFNAR1/2 on NK cells^{32 33} and indirectly through induction of IL-15 expression in cDCs.¹³ Frequencies of the cytotoxic and more mature CD11b⁺CD27⁺ effector NK subset were significantly reduced and those of less cytotoxic, CD11b⁺CD27⁻ and

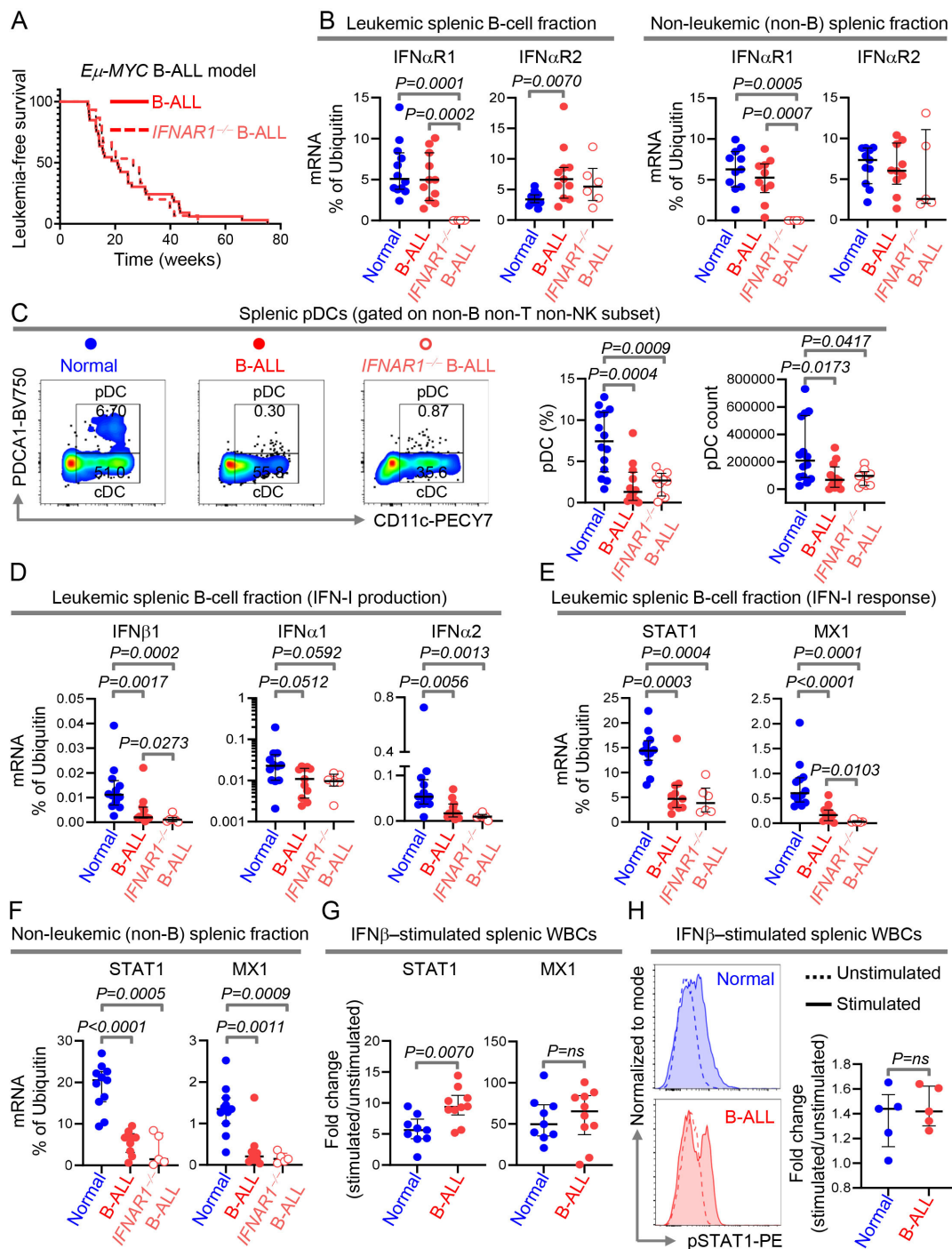


Figure 2 Intrinsic suppression of IFN-I production is sufficient to drive overt B-cell leukemogenesis. (A) Comparison of leukemia-free survival between *IFNAR1*^{+/-} B-ALL-bearing (n=33) and *IFNAR1*^{-/-} B-ALL-bearing (n=15) *Eμ*-Myc mice. (B) Quantitation of *IFNAR1* and *IFNAR2* transcript expression by qPCR in MACS sorted splenic B- and non-B cell fraction of wildtype (normal, B cell fraction, n=12; non-B cell fraction, n=11), *IFNAR1*^{+/-} *Eμ*-Myc B-ALL-bearing (B cell fraction, n=11; non-B cell fraction, n=10) and *IFNAR1*^{-/-} *Eμ*-Myc B-ALL-bearing (B cell fraction, n=6; non-B cell fraction, n=5) mice. (C) Comparison of splenic pDC numbers and representative flow cytometry plots of normal (n=14), *IFNAR1*^{+/-} *Eμ*-Myc B-ALL-bearing (n=12) and *IFNAR1*^{-/-} *Eμ*-Myc B-ALL-bearing (n=10) mice. (D–F) Quantitation of transcripts of *IFNβ1*, *IFNα1* and *IFNα2* in splenic B cells (D), and *STAT1* and *MX1* in splenic B- and non-B cell fractions (E, F) by qPCR. (G) Fold change in induction of *STAT1* and *MX1* transcripts after *IFNβ* stimulation in splenic WBCs of normal (n=9) and *IFNAR1*^{+/-} *Eμ*-Myc B-ALL-bearing (n=10) mice. (H) Histogram overlays and scatter plot showing the MFI and fold increase in MFI after *IFNβ* stimulation in splenic WBC from normal (n=5) and *IFNAR1*^{+/-} *Eμ*-Myc B-ALL-bearing mice (n=5). Ubiquitin (UB) was used as housekeeping gene in qPCR. For all flow cytometry experiments, one representative dot plot from each group is shown. Survival was calculated by Kaplan-Meier method and p value calculated by log-rank test. All other comparisons between any two groups were conducted using Mann-Whitney U test. Exact p values are provided whenever significant (<0.05) or trending to significance (0.05<p<0.1). B-ALL, B-cell acute lymphoblastic leukemia; MFI, median fluorescence intensity; pDC, plasmacytoid dendritic cell; WBCs, white blood cells.

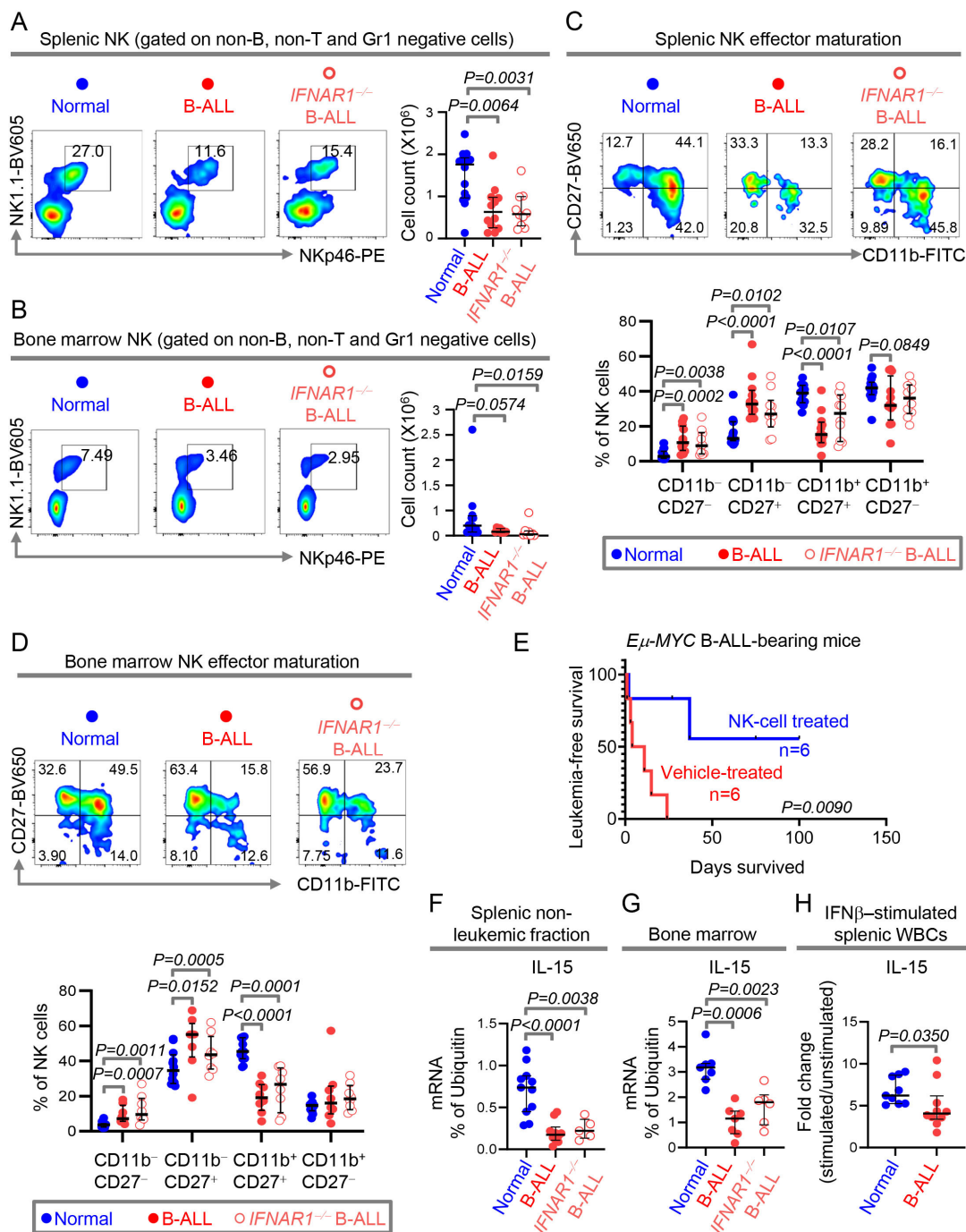


Figure 3 Reduced IFN-I production in B-ALL is sufficient to suppress IL-15 and systemically impair NK surveillance. (A, B) Comparison of NK cell counts and representative plots of NK frequencies within the non-B, non-T and Gr1 negative cell fractions of the spleen (A) and bone marrow (B) of normal (spleen, $n=14$; bone marrow, $n=12$), *IFNAR1*^{+/+} *Eμ*-Myc B-ALL-bearing (spleen, $n=12$; bone marrow, $n=8$) and *IFNAR1*^{-/-} *Eμ*-Myc B-ALL-bearing (spleen, $n=10$; bone marrow, $n=8$) mice. (C, D) Comparison of frequencies of NK subsets within the four-stage NK-cell effector maturation pathway in spleen (C) and bone marrow (D) of normal (spleen, $n=14$; bone marrow, $n=12$), *IFNAR1*^{+/+} *Eμ*-Myc B-ALL-bearing (spleen, $n=12$; bone marrow, $n=8$) and *IFNAR1*^{-/-} *Eμ*-Myc B-ALL-bearing (spleen, $n=10$; bone marrow, $n=8$) mice. (E) Comparison of leukemia-free survival between *Eμ*-Myc B-ALL-bearing mice treated with vehicle control or with syngeneic NK cells ($n=6$, each group). (F–H) Quantitation of IL-15 transcript expression by qPCR in MACS sorted splenic non-B cell fraction (F) and total bone marrow (G) of wildtype (normal, spleen, $n=11$; bone marrow, $n=7$), *IFNAR1*^{+/+} *Eμ*-Myc B-ALL-bearing (spleen, $n=10$; bone marrow, $n=7$) and *IFNAR1*^{-/-} *Eμ*-Myc B-ALL-bearing (spleen, $n=5$; bone marrow, $n=6$) mice. (H) Fold change in induction of IL-15 transcript in IFN β -stimulated splenic WBCs of normal ($n=9$) and *IFNAR1*^{+/+} *Eμ*-Myc B-ALL-bearing ($n=10$) mice. Ubiquitin (UB) was used as housekeeping gene in qPCR. For all flow cytometry experiments, one representative dot plot from each group is shown. All other pairwise comparisons between any two groups were conducted using Mann-Whitney U test. Exact p values are provided whenever significant (<0.05) or trending to significance ($0.05 < p < 0.1$). B-ALL, B-cell acute lymphoblastic leukemia; NK, natural killer; WBCs, white blood cells.

CD11b⁺CD27⁺ immature NK fractions were significantly increased in spleen and BM of B-ALL mice independent of *IFNAR1* genotype (figure 3C,D). These observations suggested that NK cell-based therapies would be attractive to overcome the intrinsic suppression of IFN-I production in B-ALL. As predicted, administration of syngeneic healthy NK cells prolonged leukemia-free survival of B-ALL-bearing *Eμ-MYC* mice compared with their counterparts who received no NK cells (figure 3E, online supplemental figure S12).

In a transgenic mouse model of IFN-I^{low}, MYC-inducible primary T-ALL, we showed that administration of IFN-Is restores NK surveillance and improves survival and NK cells mediate IFN-I's anti-leukemic effects.⁹ To determine the extent to which reduced IFN-I production drives NK suppression in B-ALL, we administered IFNβ to B-ALL-prone *Eμ-MYC* mice aged 7–20 weeks for 9 days. In each mouse, we measured the fold change in percentages of NK cells, NK-cell effectors, and B-cells (ALL) before and after administration of PBS (control) or IFNβ. Administration of IFNβ to B-ALL prone mice reduces the leukemia progression and increases the frequencies of total NK cells and cytotoxic CD27⁺CD11b⁺ NK-cell effectors in circulation (online supplemental figure S13). Changes we find induced in NK subsets after IFNβ administration phenocopy those shown to be induced by IL-15 treatment.³⁴

IL-15 is an IFN-I-induced cytokine indispensable for NK-cell survival, proliferation, effector maturation, and immune surveillance.^{13 35} IL-15 expression in splenic non-leukemic fraction and total BM of both *IFNAR1*^{+/+} and *IFNAR1*^{-/-} B-ALL-bearing mice was equally reduced (figure 3E,G), strengthening our observations that *IFNAR1* loss does not worsen NK suppression in B-ALL. Next, we determined the extent to which ex vivo addition of IFN-Is to splenic leukocytes from B-ALL mice can stimulate IL-15 transcription in B-ALL. IFN-I treatment induced IL-15, although to a lesser extent in the B-ALL microenvironment compared with their healthy counterparts (figure 3H). We speculate that the inability of ex vivo IFN-I stimulation to induce IL-15 production to the same extent in B-ALL and normal splenic microenvironments (figure 3H) could result from alterations in IFN-I-responsive, IL-15-producing cDCs in B-ALL.

Overall, natural suppression of IFN-I production during B-leukemogenesis is sufficient to systemically suppress IL-15 expression and impair NK surveillance. NK cell-based therapies^{16 36 37} thus represent a good therapeutic strategy to overcome the intrinsic suppression of IFN-I and IL-15-induced NK surveillance in B-ALL.

Expression of IL-15 inversely correlates with MYC expression in human B-cell malignancies

We showed suppressed NK-cell numbers and effector maturation in patients with B-ALL.¹² Together with the intrinsic suppression of IFN-I production in B-ALL patients (figure 1), our findings¹² suggested that the IFN-I-induced, NK surveillance-activating cytokine, IL-15,^{13 35}

may be reduced in patients with B-ALL. Unfortunately, antibodies to compare human IL-15 protein expression in healthy individuals and B-ALL patients are unavailable.³⁸ As a surrogate for IL-15 expression, we compared frequencies of potential IL-15-producing cDCs within the non-leukemic fraction of B-ALL patients and healthy donors. cDCs were significantly reduced in PBMC of B-ALL patients (figure 4A). Reduced pDC-derived IFN-Is and cDC-derived, IFN-I-induced cytokine, IL-15, suggest IL-15-producing NK cells may be therapeutically efficacious in B-ALL.^{36 39}

We asked whether IL-15 is differentially suppressed across the B-ALL subtypes with widely divergent outcomes. To this end, we compared the expression of IL-15 transcripts in major subgroups of childhood and adult B-ALL from three independent datasets.^{4 20 21 40–42} IL-15 expression was significantly reduced in patients with *MYC* or *BCL2* translocations, *KMT2A*-rearrangements, and hypodiploidy in comparison to *Ph*⁺, *Ph-like*, and *ETV6::RUNX1* subtypes (figure 4B). Expression of IL-15 correlated negatively with MYC expression in B-ALL subtypes (figure 4B). The converse relationship between IL-15 and MYC expression was validated in B-cell lymphomas: classical MYC-driven burkitt's lymphoma (BL) expressed lower IL-15 than other subtypes (figure 4C). These observations are concordant with our previous findings that MYC directly represses IFN-I signaling.⁹ We infer that strong suppression of IL-15 in MYC-overexpressing human B-ALLs might render them particularly sensitive to the administration of NK cell-based therapies, as shown in mice in figure 3E.

CRISPRa-engineered IL-15-secreting NK cells eradicate MYC-overexpressing B-ALLs in vitro

IL-15-producing NK therapies were found to be effective in preclinical studies and clinical trials of AML, chronic lymphocytic leukemia (CLL), and BL.^{36 39 43} We investigated whether IL-15-producing NK cells are also efficacious in eradicating human B-ALL, specifically B-ALL subtypes characterized by high MYC expression. To engineer IL-15-producing NK cells for proof-of-concept studies, we used CRISPRa to transcriptionally activate IL-15 in the NK-cell line, NK-92.¹⁶ CRISPRa-mediated transcriptional activation of IL-15 in human NK cells has advantages over lentiviral overexpression.^{36 43} First, it is easier to introduce a ~20 nt sgRNA to activate IL-15 transcription by CRISPRa as opposed to transducing NK cells with an overexpression vector encoding IL-15. Second, IL-15 transcript levels increase by ~3-fold and secreted IL-15 is 2 pg/mL in CRISPRa IL-15 NK cells (figure 5A), which is much lower than that seen in NK cells engineered to overexpress IL-15.^{36 43} Hence, cellular toxicity caused by excessive production of IL-15⁴³ can be avoided in CRISPRa.

CRISPRa-IL-15-NK cells are comparable in their properties and functionality to NK cells overexpressing IL-15.⁴³ Transcriptional activation of IL-15 improved the proliferation of IL-2-dependent NK-92 cells in the presence

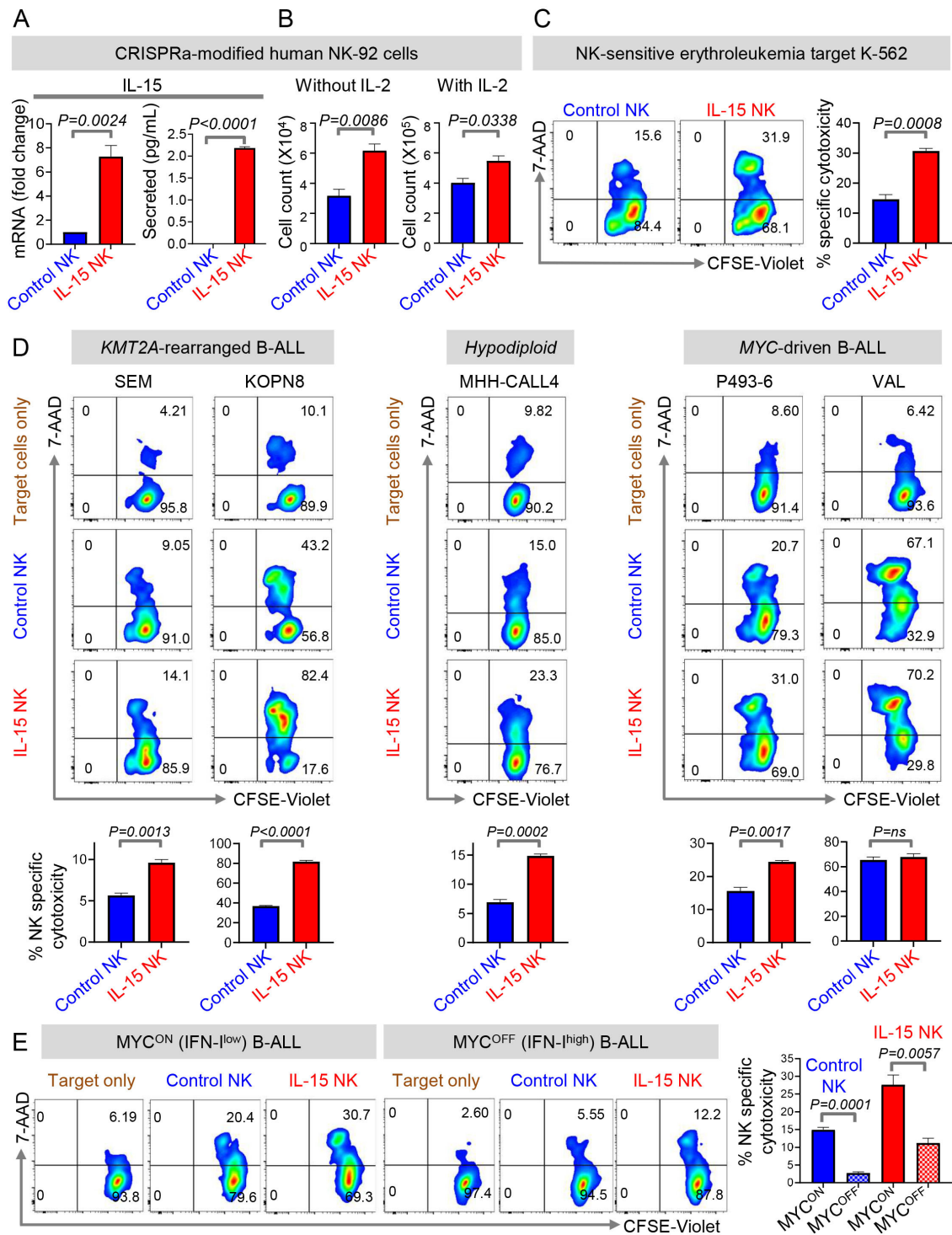


Figure 5 CRISPRa-engineered IL-15 secreting NK cells eradicate MYC-overexpressing B-ALLs in vitro. (A) Fold change in IL-15 transcript levels by qPCR in dCas9-VP64-GFP⁺ NK-92 cells transduced with control sgRNA-RFP (Control NK) or IL-15 sgRNA-RFP (IL-15 NK) and levels of secreted IL-15 by ELISA in culture supernatant of control NK and IL-15 NK cells stimulated with PMA and Ionomycin for 24 hours. (B) Cell counts of control and IL-15 NK cells cultured in the presence and absence of rhIL-2 (100 U/mL) for 96 hours. (C, D) Specific cytotoxicity of control and IL-15 NK cells by flow cytometry using (C) K562, (D) SEM (KMT2A-rearranged), KOPN8 (KMT2A-rearranged), MHH-CALL4 (hypodiploid, CRLF2-rearranged), P493-6, and VAL as target cell lines. Effector: target=10:1. (E) Specific cytotoxicity of control and IL-15 NK cells by flow cytometry against MYC-overexpressing (MYC^{ON}) and MYC-inactivated (MYC^{OFF}) P493-6 cells. MYC was inactivated by treatment of P493-6 cells with 0.2 μ g/mL of doxycycline for 24 hours. $p=0.0108$, control (MYC^{ON}) vs IL-15 NK (MYC^{ON}); $p=0.0037$, control (MYC^{OFF}) vs IL-15 NK (MYC^{OFF}). All experiments were conducted in three technical and three biological replicates. One representative of three biological replicates of each experiment is shown. Comparisons between any two groups were conducted using Student's t-test (A–E). Exact p values are provided whenever significant (<0.05) or trending to significance ($0.05<p<0.1$). B-ALL, B-cell acute lymphoblastic leukemia; NK, natural killer; ns, not significant.

with their MYC^{ON} (IFN-I^{low}) counterparts. However, the enforced expression of IL-15 in NK cells significantly enhanced its potential to kill both MYC^{ON} (IFN-I^{low}) and MYC^{OFF} (IFN-I^{high}) B-lymphoblasts (figure 5E). Thus, MYC overexpression is at least one factor that sensitizes B-lymphoblasts to NK cell-based therapies. CRISPRa-engineered IL-15 NK cells thus represent a potentially safe and particularly efficacious approach to treat poor prognosis MYC-overexpressing, IFN-I^{low} B-ALLs.

CRISPRa-engineered IL-15-secreting NK cells slow down progression of MYC-overexpressing B-ALL in vivo

We strengthened the therapeutic potential of IL-15-producing NK cells in poor prognosis MYC-overexpressing B-ALL by comparing the in vivo efficacy of CRISPRa-engineered IL-15 human NK cells and control NK cells in a cell-line derived xenograft model of human MYC-driven B-lymphoblasts. We transplanted luciferase-labeled MYC-overexpressing malignant human B cells into immune deficient NSG mice. After confirming B-lymphoblast engraftment by BLI, we administered CRISPRa-control or CRISPRa-IL-15 NK cells and compared disease progression between the two groups by BLI (figure 6A). CRISPRa IL-15-secreting NK cells significantly slowed down progression and spread of engrafted human B-lymphoblasts compared with control NK cells in vivo (figure 6B,C). Thus, IL-15-producing NK cells warrant extensive preclinical and clinical studies for the treatment of high-risk B-ALL subgroups that overexpress MYC.

DISCUSSION

Via these studies, we provide new evidence for the natural suppression of IFN-I production during primary murine and human B-cell leukemogenesis. In addition to reduced IFN-I transcription by malignant B cells seen here and in our earlier studies,⁹ we find pDC-derived paracrine IFN-I production is reduced in patients and mice with B-ALL. This blockade in the first step of the IFN-I pathway is sufficient to drive leukemogenesis and overrides any additional downstream disruption of the IFN-I pathway such as, ablation of *IFNARI* shown here. The clinical relevance of IFN-I suppression in human B-ALL is underscored by the favorable prognosis of B-ALL patients who express high levels of ISGs.

Our comparisons in *IFNARI*^{+/+} and *IFNARI*^{-/-} B-ALL-bearing mice suggest that suppression of IFN-I production is likely caused by B-lymphoblasts. We previously showed that MYC suppresses IFN-I production by malignant cells and blocks NK surveillance in an MYC-inducible T-ALL mouse model.⁹ Similarly, MYC-induced signaling in B-lymphoblasts may perturb cytokines required for pDC differentiation in B-ALL. Another explanation for reduction of pDCs in B-ALL microenvironments could be the MYC-driven accumulation of B-lymphoid precursors thereby suppressing the lymphoid lineage pDCs.⁴⁴ However, reduction in myeloid pDCs cannot be ruled out especially given the plasticity between the lymphoid and

myeloid pDCs.⁴⁴ How oncogenic pathways perturb pDC homeostasis remains to be explored.

Among non-leukemic host immune cells, NK cells are maximally impacted by the suppressed IFN-I production in B-ALL likely because of the reduced synthesis of IL-15 by IFN-I-responding cDCs. While ex vivo treatment of primary B-ALL samples with IFN-Is fully rescues proximal IFN-I signaling, its partial induction of IL-15 was possibly due to absence or functional suppression of cDCs. Further studies are needed to delineate the mechanisms underlying the suppression of cDCs in B-ALL. As with suppression of NK surveillance shown by us,¹² we speculate that oncogenic pathways in leukemia cells may drive suppression of cDCs in ALL.

Our results partly explain why IFN-Is are effective when administered to acute leukemia patients who undergo allogeneic BM transplantation^{10 11 45}; intrinsically suppressed IFN-I production in B-ALL may reduce IFN-I-dependent anti-leukemia immune subsets, including NK cells and cDCs, thereby rendering single agent IFN-I therapy ineffective. We maintain that IL-15-producing NK cells, represent a novel, effective, and affordable approach to achieve the combined therapeutic benefits of IFN-I administration and BM transplantation for several reasons: (1) graft versus leukemia effects in allogeneic transplants are known to be largely mediated by NK cells,⁴⁶ (2) allogeneic NK cell-based therapies do not induce graft-vs-host disease, cytokine release syndrome, or neurotoxicity,⁴⁷ and (3) and we find suppressed IL-15 production and NK surveillance to be the most striking consequences of IFN-I loss in B-ALL.

Our studies suggest that CRISPRa-engineered IL-15-producing NK cells represent an efficacious and potentially safe approach to reverse the detrimental effects of suppressed IFN-I, IL-15 production and NK surveillance in high-risk B-ALL (graphical abstract). While IL-15-producing NK cells were shown to be effective in preclinical studies of AML, CLL, and BL,^{36 39 43} we are the first to delineate the biology underlying its efficacy in B-ALL and demonstrate its ability to eradicate B-ALL subtypes with highest MYC and lowest IL-15 expression including MYC/BCL2-rearranged, KMT2A-rearranged, and hypodiploid. We find that MYC overexpression sensitizes B-ALLs to NK cell-mediated killing. Hence, IL-15-producing NK cells may be a viable alternative to drugging MYC in these high-grade B-ALL subtypes.⁴⁸

The lack of reliable cytometry antibodies for mouse and human intracellular IL-15³⁸ and mouse IFN-Is precluded us from measuring these proteins in specific immune subsets in the B-ALL microenvironment. This problem was mitigated for CRISPRa-IL-15-NK cells by measuring secreted IL-15 and conducting phenotypic (proliferation) and functional (cytotoxicity against NK-sensitive erythroleukemia) validation of these cells.

Because of the relative ease in constitutively expressing dCas9-VP64,¹⁶ NK-92 lymphoma cells⁴⁹ were used instead of primary NK cells to engineer CRISPRa IL-15-NK cells. CRISPRa-engineered and other primary IL-15-producing

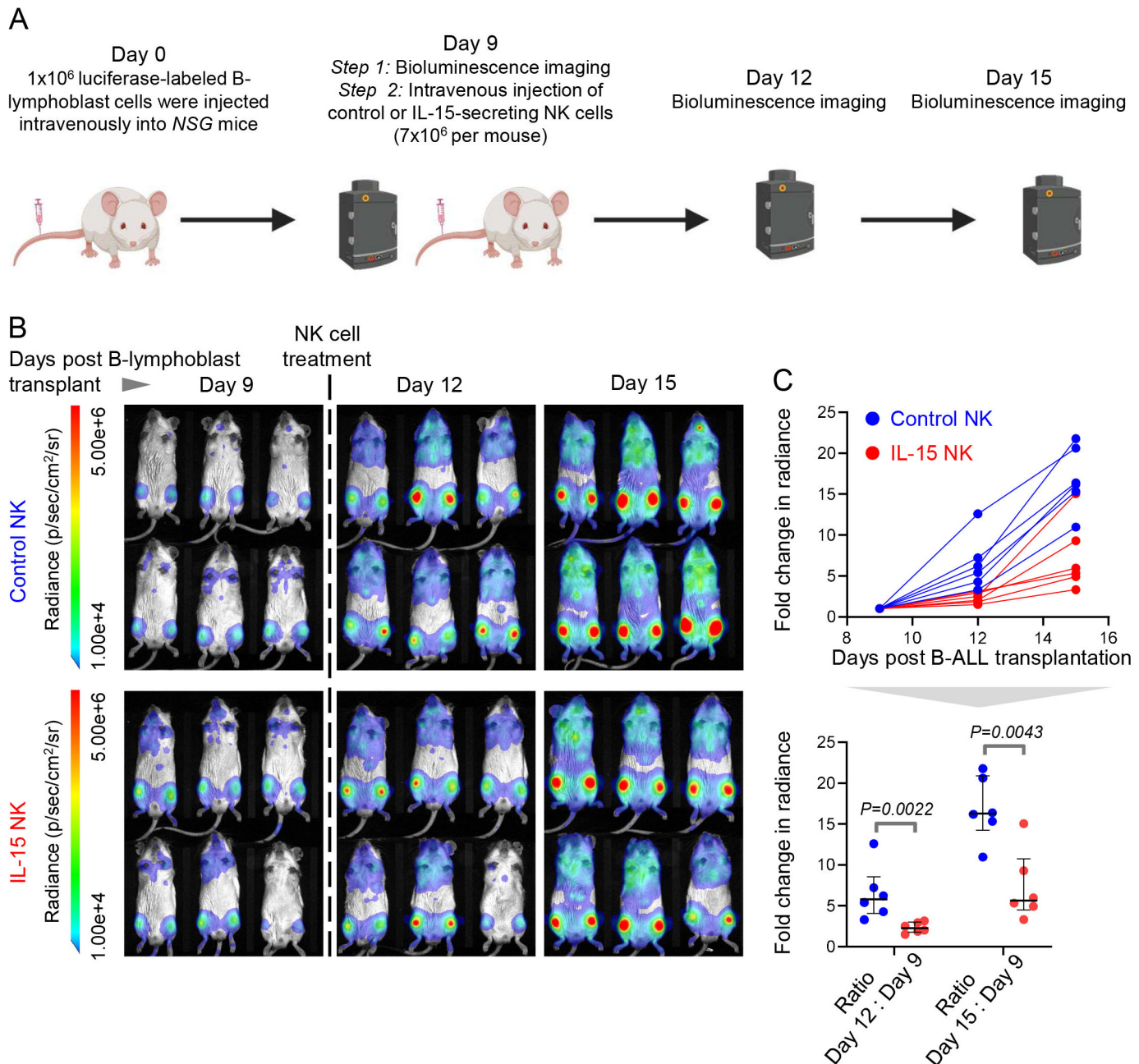


Figure 6 CRISPRa-engineered IL-15-secreting NK cells slow down progression of MYC-overexpressing B-ALL in vivo. (A) Experimental design for comparing the in vivo therapeutic efficacies of CRISPRa-engineered IL-15 producing and control NK cells in a luciferase-labeled human cell line-derived xenograft (CDX) of MYC-driven B-cell malignancy (P493-6). Schematic was created using BioRender.com. (B) Bioluminescence imaging of leukemia progression in *NOD-SCID IL2R γ ^{-/-}* (NSG) CDX recipients before (day 9 post-CDX transplantation) and after treatment with control and IL-15 NK cells (days 12 and 15 post-CDX transplantation) (n=6 mice each in control NK and IL-15 NK arms). (C) Quantification of fold change in full body bioluminescence (photons/sec/cm²/sr) on days 12 and 15 post B-lymphoblast transplantation in control-NK (n=6) and IL-15-NK- treated (n=6) CDX recipients. P values were calculated by Mann-Whitney U test. Exact significant p values (<0.05) are provided. B-ALL, B-cell acute lymphoblastic leukemia; NK, natural killer.

NK cell-based therapies therefore await further preclinical and clinical development. In this study, we did not measure the efficacy of IL-15-secreting human NK cells in prolonging survival of mice bearing B-ALL xenografts. Such studies would require repeat injections of the IL-15 NK cells or their further manipulation to increase persistence in human ALL xenograft-bearing mice. Nevertheless, our current mechanistic findings will

accelerate the development of primary IL-15-producing NK therapies^{37 50} for sustaining remission of hard-to-treat human B-ALL.

Author affiliations

¹Department of Systems Biology, City of Hope Beckman Research Institute, Monrovia, California, USA

²The Human Immune Monitoring Center (HIMC), Institute for Immunity, Transplantation and Infection, Stanford University School of Medicine, Stanford, California, USA

³The Hematopoietic Tissue Biorepository/Research Pathology Shared Resources, City of Hope, Duarte, California, USA

⁴Department of Pediatrics, Stanford University School of Medicine, Stanford, California, USA

⁵Department of Hematology and Hematopoietic Cell Transplantation, City of Hope National Medical Center, Duarte, California, USA

⁶Department of Cancer and Cellular Biology, Fels Cancer Institute for Personalized Medicine Temple University Lewis Katz School of Medicine, Philadelphia, Pennsylvania, USA

⁷Department of Medicine, University of Pennsylvania Perelman School of Medicine, Philadelphia, Pennsylvania, USA

⁸Department of Pediatrics, Division of Oncology, The Children's Hospital, Philadelphia, Pennsylvania, USA

⁹Hematological Malignancies Translational Science, City of Hope, Duarte, California, USA

¹⁰Department of Pediatrics, City of Hope, Duarte, California, USA

¹¹Hematology-Oncology Department, Tel Aviv University, Tel Aviv, Israel

Twitter Anil Kumar @anilsharma085 and Srividya Swaminathan @sswamin17

Acknowledgements We thank the Hematopoietic Tissue Biorepository (HTB) of City of Hope, the Bass Center for Childhood Cancer and Blood Diseases at Stanford University, and the Stem Cell and Xenograft Core (SCXC) at the University of Pennsylvania for providing us primary B-ALL patient specimens. We thank the staff at the Human Immune Monitoring Center at Stanford University and at the Analytical Cytometry Core of the City of Hope. We thank Dr. Mark Davis (Stanford University) for access to PBMCs from an influenza vaccine study and Dr. Eleanora Heisterkamp (City of Hope) for providing us K562 cells for conducting in vitro cytotoxicity experiments. Schematics were created using BioRender.com.

Contributors AK conducted most of the experiments, analyzed data, and interpreted the results. ATK conducted experiments and analyzed clinical data from publicly available B-ALL datasets. CD conducted CyTOF-based immune profiling of patient samples, analyzed data, and interpreted the results. SA assisted AK with NK cell therapy adoptive transfer experiments in primary mouse models. ASO, SJL and AC assisted AK with CRISPR-based NK-cell modifications. TM and MH collected, processed and curated samples from consented B-ALL patients used for flow cytometry and CyTOF. KMS, NJL, MC, SKT, LG and GM provided access to fully deidentified coded samples with associated clinical annotation collected on IRB-approved research protocols. JY and MAC provided guidance on NK-cell biology. KMS, NJL, MC, SKT, GM, LG, CH, SA, STR, SI and ZG provided scientific input on ALL biology, immune microenvironment in ALL, and/or IFN- γ signaling. CW-C provided guidance on CRISPR. All authors edited the manuscript. SS, SJF and HTM provided scientific guidance, administrative, technical, and material support. SS conceived the study, developed the experimental methodology, interpreted the results, wrote the manuscript, and supervised the study. SS is responsible for the overall content as guarantor.

Funding This work was supported by the following grants: Special Fellow (LLS 3366-17) and Translational Research Program (LLS 6624-21) Awards from The Leukemia and Lymphoma Society (SS), American Society of Hematology Scholar Award (SS), PhRMA Foundation Research Starter Grant in Drug Discovery (SS), Childhood Cancer Research Grant from the Andrew McDonough B+ Foundation (SS), City of Hope Chancellor's Research Grant (SS), P50 CA107399-12 National Cancer Institute-City of Hope Lymphoma SPORE Career Enhancement Program Pilot Award from the National Institutes of Health (PIs: SJF and Larry Kwak, Pilot Awardee: SS), a Research Start-Up Budget from the Beckman Research Institute of the City of Hope (SS), and 1U24CA224309 from the National Institutes of Health (HTM). The Hematopoietic Tissue Biorepository and Analytical Cytometry Core at the City of Hope are Shared Resource Cores supported by the National Cancer Institute of the National Institutes of Health under grant number P30CA033572. SKT is a Scholar of the Leukemia and Lymphoma Society and holds the Joshua Kahan Endowed Chair in Pediatric Leukemia Research at the Children's Hospital of Philadelphia. SI is supported by the Israel Cancer Research Fund, City of Hope and Professorship award. CH is supported by NCI 5K22CA251649-02, Rally Foundation for Childhood Cancer, V Foundation for Cancer Research, and the Leukemia Research Foundation.

Disclaimer The content is solely the responsibility of the authors and does not necessarily represent the official views of the National Institutes of Health.

Competing interests The work described in this study is covered by pending US and PCT patent applications assigned to City of Hope and/or Stanford University with inventors SS, AK, ATK, CW-C, SJL, CD and HTM. MAC and JY are cofounders of Cytolimmune Therapeutics.

Patient consent for publication Not applicable.

Ethics approval Mice were purchased from Jackson Laboratories and maintained in the City of Hope's laboratory animal resource facility under approval of Institutional Animal Care and Use Committee (IACUC 19032). This study is classified as non-human subjects research under the City of Hope IRB19373.

Provenance and peer review Not commissioned; externally peer reviewed.

Data availability statement Data are available in a public, open access repository. Data are available on reasonable request. All data relevant to the study are included in the article or uploaded as online supplemental information. GSE numbers are indicated for all analyses involving previously published microarray and RNA sequencing data sets in figure legends. The following information has been provided for the deidentified B-ALL patient samples used in our study: Patient I.D., age, gender, tissue type, cytogenetics, translocation or mutation status, disease status, the originating institution, and frequencies of IFN α 2b+ cells wherever available. For mass and flow cytometry-based immune cell profiling, we have provided details of markers, labels, and gating strategy in Supplemental Information. We have also provided detailed protocols for all experiments and analyses in the Methods Section of the manuscript. Renewable materials can be obtained by directly contacting the corresponding author at sswaminathan@coh.org.

Supplemental material This content has been supplied by the author(s). It has not been vetted by BMJ Publishing Group Limited (BMJ) and may not have been peer-reviewed. Any opinions or recommendations discussed are solely those of the author(s) and are not endorsed by BMJ. BMJ disclaims all liability and responsibility arising from any reliance placed on the content. Where the content includes any translated material, BMJ does not warrant the accuracy and reliability of the translations (including but not limited to local regulations, clinical guidelines, terminology, drug names and drug dosages), and is not responsible for any error and/or omissions arising from translation and adaptation or otherwise.

Open access This is an open access article distributed in accordance with the Creative Commons Attribution Non Commercial (CC BY-NC 4.0) license, which permits others to distribute, remix, adapt, build upon this work non-commercially, and license their derivative works on different terms, provided the original work is properly cited, appropriate credit is given, any changes made indicated, and the use is non-commercial. See <http://creativecommons.org/licenses/by-nc/4.0/>.

ORCID iDs

Anil Kumar <http://orcid.org/0000-0003-2287-5388>

Caroline Duault <http://orcid.org/0000-0003-2742-1668>

Anthony Chan <http://orcid.org/0000-0002-7091-1294>

Sarah K. Tasian <http://orcid.org/0000-0003-1327-1662>

Srividya Swaminathan <http://orcid.org/0000-0002-3459-7488>

REFERENCES

- 1 Terwilliger T, Abdul-Hay M. Acute lymphoblastic leukemia: a comprehensive review and 2017 update. *Blood Cancer J* 2017;7:e577.
- 2 Aggarwal S. Targeted cancer therapies. *Nat Rev Drug Discov* 2010;9:427–8.
- 3 Kruger S, Illmer M, Kobold S, et al. Advances in cancer immunotherapy 2019 – latest trends. *J Exp Clin Cancer Res* 2019;38:1–11.
- 4 Gu Z, Churchman ML, Roberts KG, et al. PAX5-driven subtypes of B-progenitor acute lymphoblastic leukemia. *Nat Genet* 2019;51:296–307.
- 5 Zitvogel L, Apetoh L, Ghiringhelli F, et al. Immunological aspects of cancer chemotherapy. *Nat Rev Immunol* 2008;8:59–73.
- 6 Dunn GP, Bruce AT, Sheehan KCF, et al. A critical function for type I interferons in cancer immunoediting. *Nat Immunol* 2005;6:722–9.
- 7 Einav U, Tabach Y, Getz G, et al. Gene expression analysis reveals a strong signature of an interferon-induced pathway in childhood lymphoblastic leukemia as well as in breast and ovarian cancer. *Oncogene* 2005;24:6367–75.
- 8 Topper MJ, Vaz M, Chiappinelli KB, et al. Epigenetic therapy ties Myc depletion to reversing immune evasion and treating lung cancer. *Cell* 2017;171:1284–300.

- 9 Swaminathan S, Hansen AS, Heftdal LD, *et al.* Myc functions as a switch for natural killer cell-mediated immune surveillance of lymphoid malignancies. *Nat Commun* 2020;11:2860.
- 10 Visani G, Martinelli G, Piccaluga P, *et al.* Alpha-Interferon improves survival and remission duration in P-190BCR-ABL positive adult acute lymphoblastic leukemia. *Leukemia* 2000;14:22–7.
- 11 Magenau JM, Peltier D, Riwe M, *et al.* Type 1 interferon to prevent leukemia relapse after allogeneic transplantation. *Blood Adv* 2021;5:5047–56.
- 12 Duault C, Kumar A, Taghi Khani A, *et al.* Activated natural killer cells predict poor clinical prognosis in high-risk B- and T-cell acute lymphoblastic leukemia. *Blood* 2021;138:1465–80.
- 13 Ranson T, Vosshenrich CAJ, Corcuff E, *et al.* IL-15 is an essential mediator of peripheral NK-cell homeostasis. *Blood* 2003;101:4887–93.
- 14 Guimond M, Freud AG, Mao HC, *et al.* In vivo role of FLT3 ligand and dendritic cells in NK cell homeostasis. *J Immunol* 2010;184:2769–75.
- 15 Mattei F, Schiavoni G, Belardelli F, *et al.* IL-15 is expressed by dendritic cells in response to type I IFN, double-stranded RNA, or lipopolysaccharide and promotes dendritic cell activation. *J Immunol* 2001;167:1179–87.
- 16 Kumar A, Lee SJ, Liu Q, *et al.* Generation and validation of CRISPR-engineered human natural killer cell lines for research and therapeutic applications. *STAR Protoc* 2021;2:100874.
- 17 Pajic A, Spitkovsky D, Christoph B, *et al.* Cell cycle activation by c-myc in a Burkitt lymphoma model cell line. *Int J Cancer* 2000;87:787–93.
- 18 Lin D, Gupta S, Maecker HT. Mass cytometry. *Bio Protoc* 2015;5:e1370.
- 19 Kotecha N, Krutzik PO, Irish JM. Web-Based analysis and publication of flow cytometry experiments. *Curr Protoc Cytom* 2010;Chapter 10:Unit10.
- 20 Kang H, Chen I-M, Wilson CS, *et al.* Gene expression classifiers for relapse-free survival and minimal residual disease improve risk classification and outcome prediction in pediatric B-precursor acute lymphoblastic leukemia. *Blood* 2010;115:1394–405.
- 21 Harvey RC, Mullighan CG, Wang X, *et al.* Identification of novel cluster groups in pediatric high-risk B-precursor acute lymphoblastic leukemia with gene expression profiling: correlation with genome-wide DNA copy number alterations, clinical characteristics, and outcome. *Blood* 2010;116:4874–84.
- 22 Honda K, Yanai H, Negishi H, *et al.* Irf-7 is the master regulator of type-I interferon-dependent immune responses. *Nature* 2005;434:772–7.
- 23 Wysocka M, Zaki MH, French LE, *et al.* Sézary syndrome patients demonstrate a defect in dendritic cell populations: effects of CD40 ligand and treatment with GM-CSF on dendritic cell numbers and the production of cytokines. *Blood* 2002;100:3287–94.
- 24 Ghanem MH, Shih AJ, Khalili H, *et al.* Proteomic and single-cell transcriptomic dissection of human plasmacytoid dendritic cell response to influenza virus. *Front Immunol* 2022;13:814627.
- 25 Chopin M, Preston SP, Lun ATL, *et al.* Runx2 mediates plasmacytoid dendritic cell egress from the bone marrow and controls viral immunity. *Cell Rep* 2016;15:866–78.
- 26 Gessani S, Conti L, Del Cornò M, *et al.* Type I interferons as regulators of human antigen presenting cell functions. *Toxins (Basel)* 2014;6:1696–723.
- 27 Simmons DP, Wearsch PA, Canaday DH, *et al.* Type I IFN drives a distinctive dendritic cell maturation phenotype that allows continued class II MHC synthesis and antigen processing. *J Immunol* 2012;188:3116–26.
- 28 Longhi MP, Trumpfheller C, Idoyaga J, *et al.* Dendritic cells require a systemic type I interferon response to mature and induce CD4+ Th1 immunity with poly IC as adjuvant. *J Exp Med* 2009;206:1589–602.
- 29 Diamond MS, Kinder M, Matsushita H, *et al.* Type I interferon is selectively required by dendritic cells for immune rejection of tumors. *J Exp Med* 2011;208:1989–2003.
- 30 Dang CV, Reddy EP, Shokat KM, *et al.* Drugging the undruggable cancer targets. *Nat Rev Cancer* 2017;17:502–8.
- 31 Harris AW, Pinkert CA, Crawford M, *et al.* The E mu-myc transgenic mouse. A model for high-incidence spontaneous lymphoma and leukemia of early B cells. *J Exp Med* 1988;167:353–71.
- 32 Swann JB, Hayakawa Y, Zerafa N, *et al.* Type I IFN contributes to NK cell homeostasis, activation, and antitumor function. *J Immunol* 2007;178:7540–9.
- 33 Mizutani T, Neugebauer N, Putz EM, *et al.* Conditional IFNAR1 ablation reveals distinct requirements of type I IFN signaling for NK cell maturation and tumor surveillance. *Oncimmunology* 2012;1:1027–37.
- 34 Desbois M, Béal C, Charrier M, *et al.* IL-15 superagonist RLI has potent immunostimulatory properties on NK cells: implications for antitumoral treatment. *J Immunother Cancer* 2020;8:e000632.
- 35 Carson WE, Giri JG, Lindemann MJ, *et al.* Interleukin (IL) 15 is a novel cytokine that activates human natural killer cells via components of the IL-2 receptor. *J Exp Med* 1994;180:1395–403.
- 36 Liu E, Tong Y, Dotti G, *et al.* Cord blood NK cells engineered to express IL-15 and a CD19-targeted CAR show long-term persistence and potent antitumor activity. *Leukemia* 2018;32:520–31.
- 37 Ma S, Caligiuri MA, Yu J. Harnessing IL-15 signaling to potentiate NK cell-mediated cancer immunotherapy. *Trends Immunol* 2022;43:833–47.
- 38 Wang X, Zhao X-Y. Transcription factors associated with IL-15 cytokine signaling during NK cell development. *Front Immunol* 2021;12:610789.
- 39 Liu E, Marin D, Banerjee P, *et al.* Use of CAR-transduced natural killer cells in CD19-positive lymphoid tumors. *N Engl J Med* 2020;382:545–53.
- 40 Harvey RC, Mullighan CG, Chen I-M, *et al.* Rearrangement of CRLF2 is associated with mutation of JAK kinases, alteration of IKZF1, Hispanic/Latino ethnicity, and a poor outcome in pediatric B-progenitor acute lymphoblastic leukemia. *Blood* 2010;115:5312–21.
- 41 Kohlmann A, Kipps TJ, Rassenti LZ, *et al.* An international standardization programme towards the application of gene expression profiling in routine leukaemia diagnostics: the microarray innovations in leukemia study prephase. *Br J Haematol* 2008;142:802–7.
- 42 Haferlach T, Kohlmann A, Wiecek L, *et al.* Clinical utility of microarray-based gene expression profiling in the diagnosis and subclassification of leukemia: report from the International microarray innovations in leukemia Study Group. *JCO* 2010;28:2529–37.
- 43 Christodoulou I, Ho WJ, Marple A, *et al.* Engineering CAR-NK cells to secrete IL-15 sustains their anti-AML functionality but is associated with systemic toxicities. *J Immunother Cancer* 2021;9:e003894.
- 44 Fitzgeraldbocarsly P, Dai J, Singh S. Plasmacytoid dendritic cells and type I IFN: 50 years of convergent history. *Cytokine & Growth Factor Reviews* 2008;19:3–19.
- 45 Mo X-D, Zhang X-H, Xu L-P, *et al.* Ifn- α is effective for treatment of minimal residual disease in patients with acute leukemia after allogeneic hematopoietic stem cell transplantation: results of a registry study. *Biol Blood Marrow Transplant* 2017;23:1303–10.
- 46 Ruggeri L, Capanni M, Urbani E, *et al.* Effectiveness of donor natural killer cell alloreactivity in mismatched hematopoietic transplants. *Science* 2002;295:2097–100.
- 47 Kumar A, Khani AT, Swaminathan S. Harnessing natural killer cell-mediated innate immune responses for cancer treatment: advances and challenges. *Explor Res Hypothesis Med* 2022.
- 48 Orlando EJ, Han X, Tribouley C, *et al.* Genetic mechanisms of target antigen loss in CAR19 therapy of acute lymphoblastic leukemia. *Nat Med* 2018;24:1504–6.
- 49 Tang X, Yang L, Li Z, *et al.* Erratum: first-in-man clinical trial of car NK-92 cells: safety test of CD33-CAR NK-92 cells in patients with relapsed and refractory acute myeloid leukemia. *Am J Cancer Res* 2018;8:1899.
- 50 Daher M, Basar R, Gokdemir E, *et al.* Targeting a cytokine checkpoint enhances the fitness of armored cord blood CAR-NK cells. *Blood* 2021;137:624–36.

Kumar et al., Supplementary Information**Intrinsic suppression of type I interferon production underlies the therapeutic efficacy of IL-15-producing natural killer cells in B-cell acute lymphoblastic leukemia**

Supplementary Figures 1-15

Supplementary Tables 1-5

Figure S1: *Concomitant high expression of IFN-I production and IFN-I signaling/response transcripts predicts favorable clinical prognosis in patients with B-ALL.*

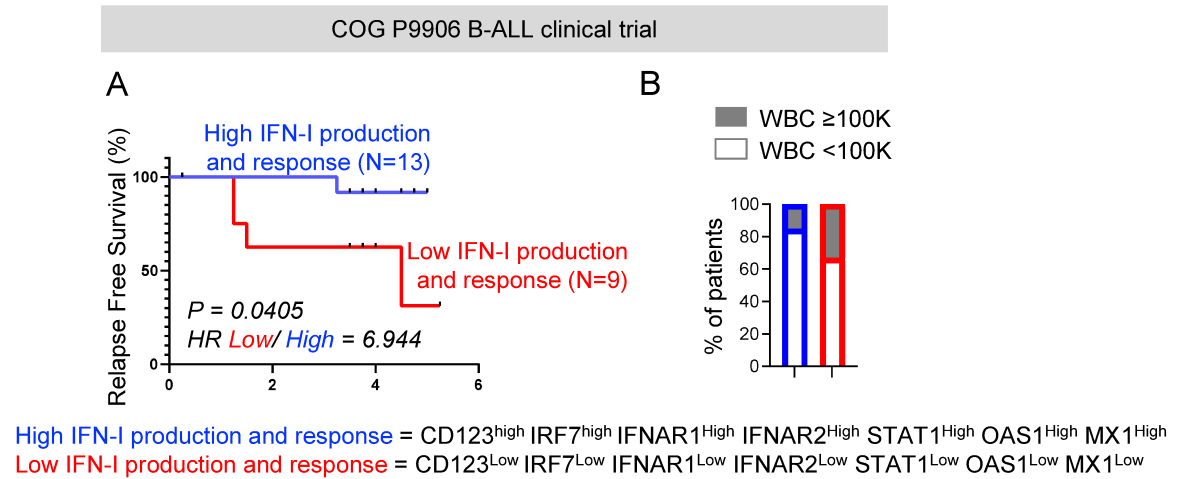


Figure S1: Concomitant high expression of IFN-I production and IFN-I signaling/response transcripts predicts favorable clinical prognosis in patients with B-ALL. (A) Comparison of survival probabilities of COG P9906 B-ALL patients separated into 2 groups based on the median transcript expressions of IFN-I production (CD123 and IRF7) and IFN-I signaling/ response (IFNAR1, IFNAR2, STAT1, OAS1, MX1) genes as ‘High IFN-I production and response’ (n=13) and ‘Low IFN-I production and response’ (n=9). (B) Stacked bar charts comparing the proportions of COG P9906 B-ALL patients with WBC count $\geq 100\,000$ or WBC count $< 100\,000$ within the ‘High IFN-I production and response’ and ‘Low IFN-I production and response’ cohorts. Survival was calculated by Kaplan-Meier method. p-value was calculated by the log-rank test. HR = Hazard ratio.

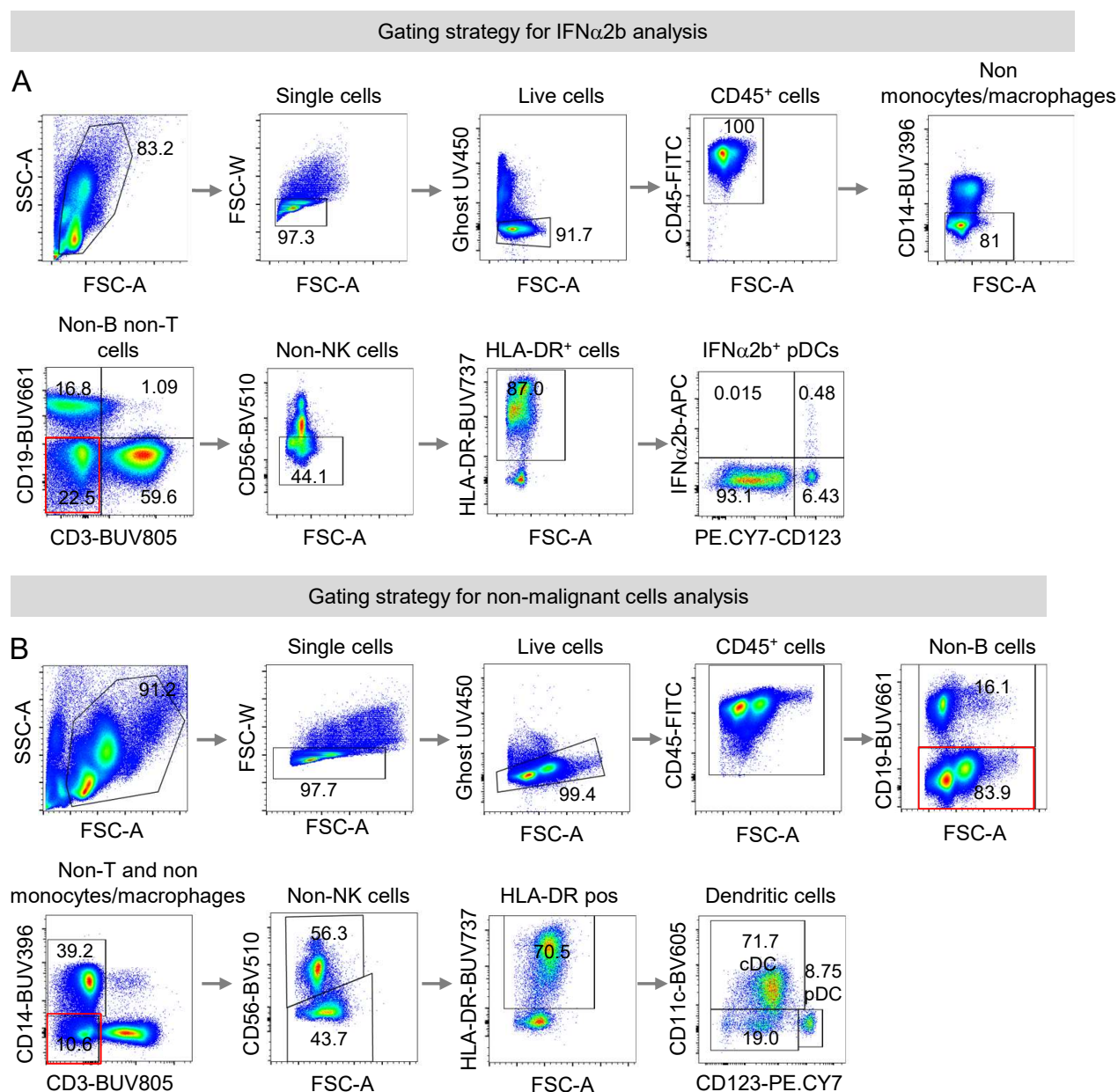
Figure S2: Gating strategy for flow cytometry analysis of human PBMCs

Figure S2: Gating strategy for flow cytometry analysis of human PBMCs. (A) For analysis of IFN α 2b-expressing immune cells, lymphocytes were gated based on forward and side scatter of the cells followed by gating of singlets and selection of live cells as Ghost-UV450⁻ and leucocytes as CD45⁺ cell fraction. Monocytes were then gated out (CD14⁻ gate), followed by selection of non-B and non-T cells (CD19⁻ CD3⁻) and non-NK cells (CD56⁻). HLA-DR⁺ cells within the ‘non-B, non-T, non-monocyte, and non-NK’ fraction were analyzed for IFN α 2b expression. **(B)** For calculating frequencies of DC subsets within the non-leukemic immune cell fraction (CD19⁻), live leucocytes were selected as in (A) followed by selection of CD19⁻ immune cells. Then HLA-DR⁺ cells were selected within non-monocytes, non-T, and non-NK cells and frequencies of cDCs, pDCs, and non-cDC/non-pDC were analyzed.

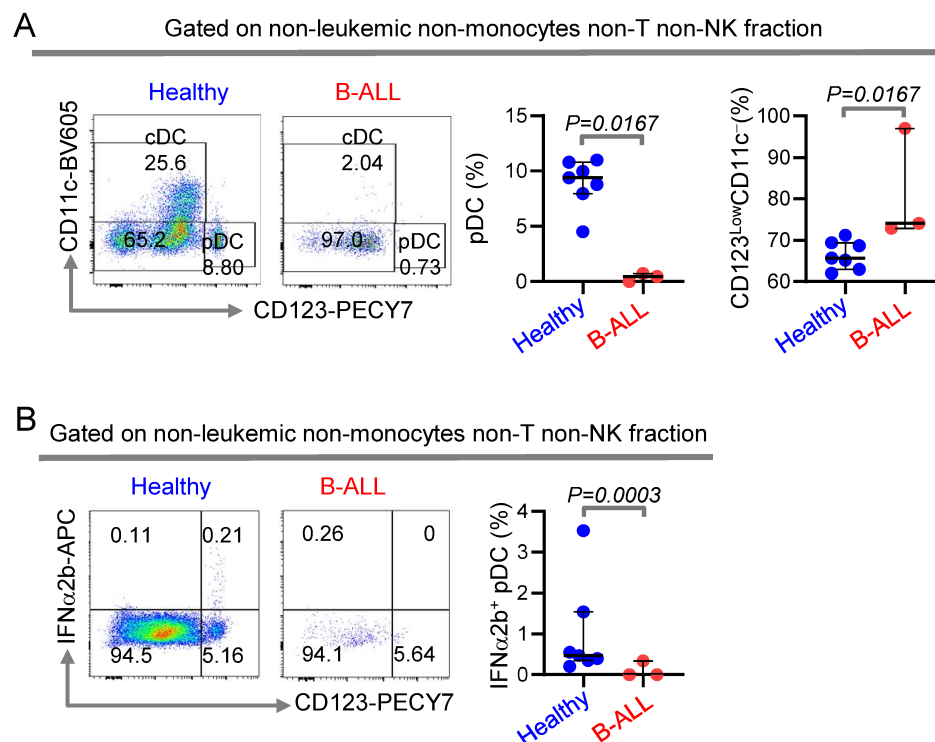
Figure S3: Reduction in frequencies of IFN-Is producers (pDC) in the BM of B-ALL patients

Figure S3: Reduction in frequencies of IFN-Is producers (pDC) in the BM of B-ALL patients (A) Comparison of bone marrow pDC frequencies within the non-B, non-monocytes, non-T, non-NK, and HLA-DR⁺ immune cell fractions between B-ALL patients (n=3) and healthy donors (n=7) by flow cytometry. **(B)** Comparison of IFN α 2b⁺ cells within the HLA-DR⁺ non-B, non-T, non-monocytes, and non-NK immune cell fraction of BMMC after stimulation with class C CpG ODN between B-ALL patients (n=3) and healthy donors (n=7) by flow cytometry. All pairwise comparisons between any two groups were conducted using the Mann-Whitney U test. Exact p-values are provided whenever significant (<0.05) or trending to significance ($0.05 < p < 0.1$).

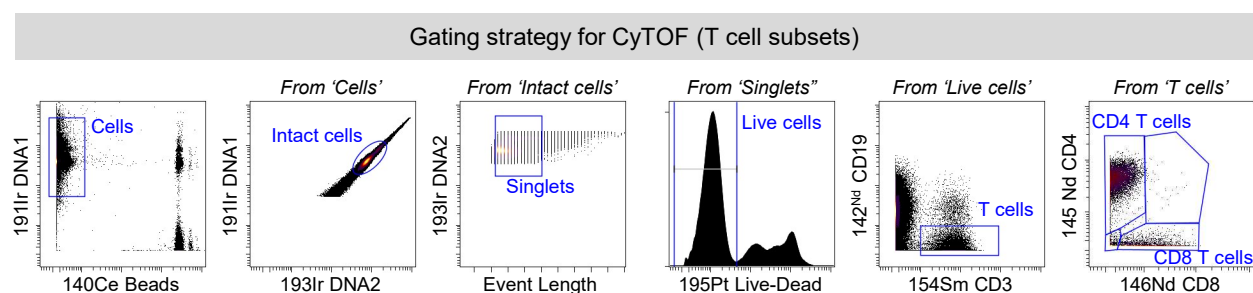
Figure S4: Gating strategy for CyTOF analysis of T-cell subsets in PBMC.**Figure S4: Gating strategy for CyTOF analysis of T-cell subsets in PBMC.** From live intact singlet populations, CD3⁺CD19⁻ cells were selected to get the non-leukemic fraction and analyzed for the frequencies of CD4⁺ and CD8⁺ cells.

Figure S5: *HLA-DR expression is reduced on leukemic B cells compared to their healthy counterparts.*

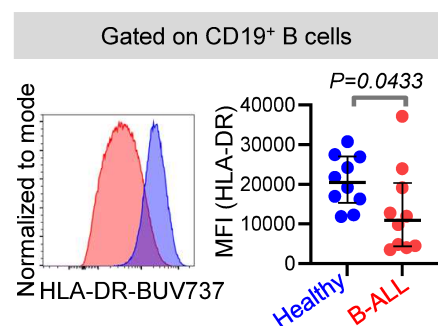


Figure S5: HLA-DR expression is reduced on leukemic B cells compared to their healthy counterparts. Representative histogram overlay and dot plots depicting median fluorescence intensity of HLA-DR expression on B cells of B-ALL patients (n=10) and healthy donors (n=10).

Figure S6: *Magnetic sorting of leukemic (B-cell) and non-leukemic (non-B) cell fractions from mouse splenic WBCs*

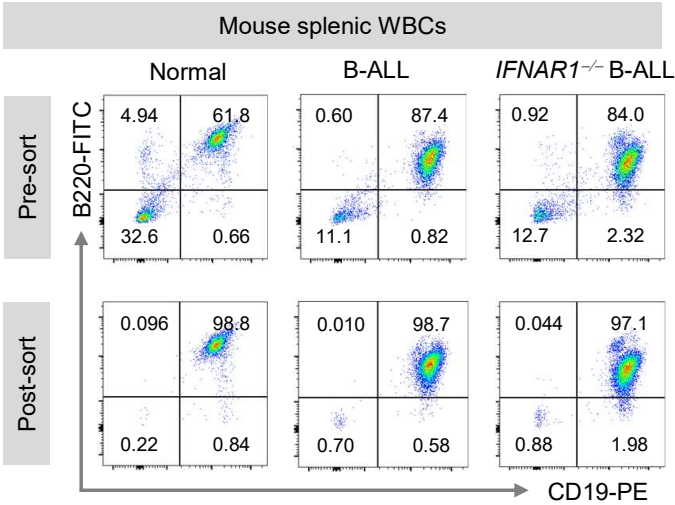


Figure S6: Magnetic sorting of leukemic (B-cell) and non-leukemic (non-B) cell fractions from mouse splenic WBCs. Representative flow cytometry plots showing the pre-sort and post-sort purity of murine splenic B-cell fractions from healthy, *Eμ-MYC* B-ALL-bearing, and *IFNAR1*^{-/-} *Eμ-MYC* B-ALL-bearing mice after magnetic-activated cell sorting.

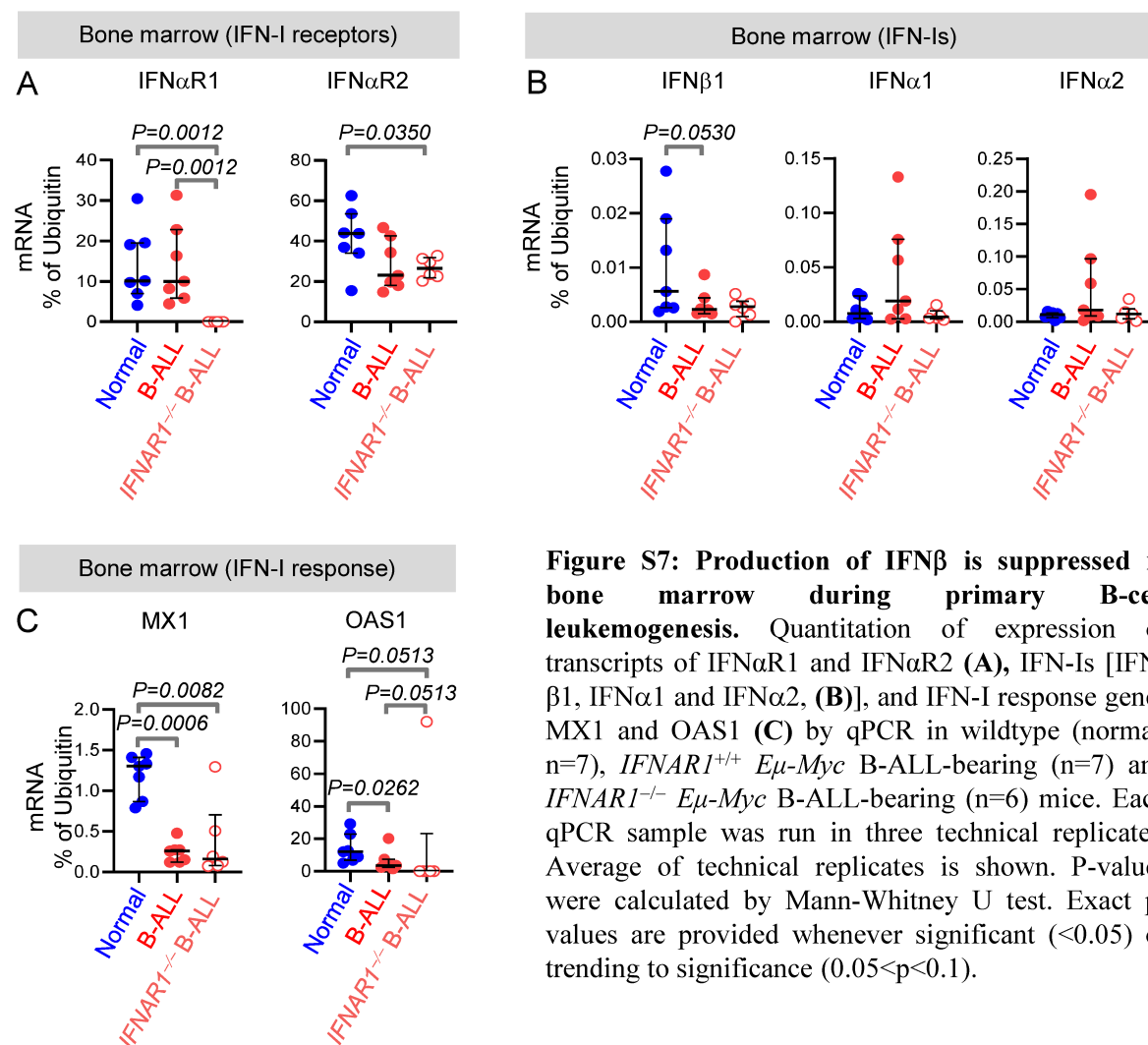
Figure S7: *Production of IFN β is suppressed in bone marrow during primary B-cell leukemogenesis*

Figure S7: Production of IFN β is suppressed in bone marrow during primary B-cell leukemogenesis. Quantitation of expression of transcripts of IFN α R1 and IFN α R2 (**A**), IFN-Is [IFN- β 1, IFN α 1 and IFN α 2, (**B**)], and IFN-I response genes MX1 and OAS1 (**C**) by qPCR in wildtype (normal, n=7), $IFNAR1^{+/+}$ *E μ -Myc* B-ALL-bearing (n=7) and $IFNAR1^{-/-}$ *E μ -Myc* B-ALL-bearing (n=6) mice. Each qPCR sample was run in three technical replicates. Average of technical replicates is shown. P-values were calculated by Mann-Whitney U test. Exact p-values are provided whenever significant (<0.05) or trending to significance (0.05<p<0.1).

Figure S8: IFN-I response is suppressed in leukemic and non-leukemic fractions during primary B-ALL development

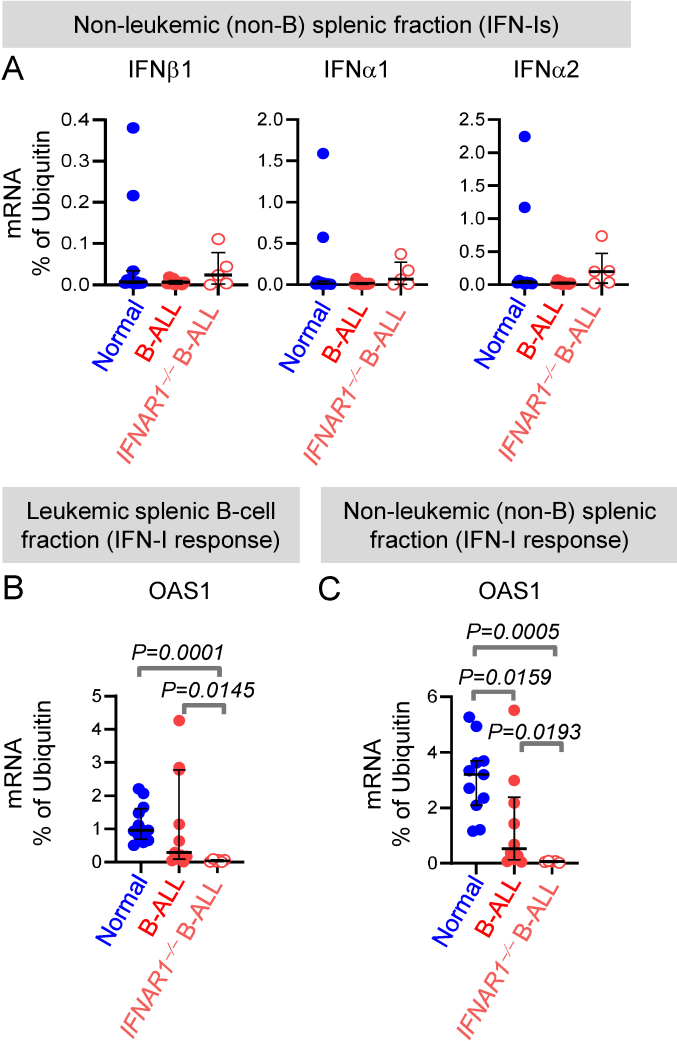


Figure S8: IFN-I response is suppressed in leukemic and non-leukemic fractions during primary B-ALL development. (A) qPCR quantitation of transcripts of IFN β 1, IFN α 1, and IFN α 2 in splenic non-B cell fraction of wildtype (normal, n=7), *IFNAR1*^{+/+} *E μ -Myc* B-ALL-bearing (spleen, n=10) and *IFNAR1*^{-/-} *E μ -Myc* B-ALL-bearing (n=5) mice. (B-C) qPCR quantitation of transcripts of OAS1 in leukemic (B) and non-leukemic (C) fractions of the spleen of wildtype (normal, n=12), *IFNAR1*^{+/+} *E μ -Myc* B-ALL-bearing (n=11) and *IFNAR1*^{-/-} *E μ -Myc* B-ALL-bearing (n=6) mice. P-values were calculated using Mann-Whitney U test. Exact p-values are provided whenever significant (<0.05) or trending to significance (0.05<p<0.1).

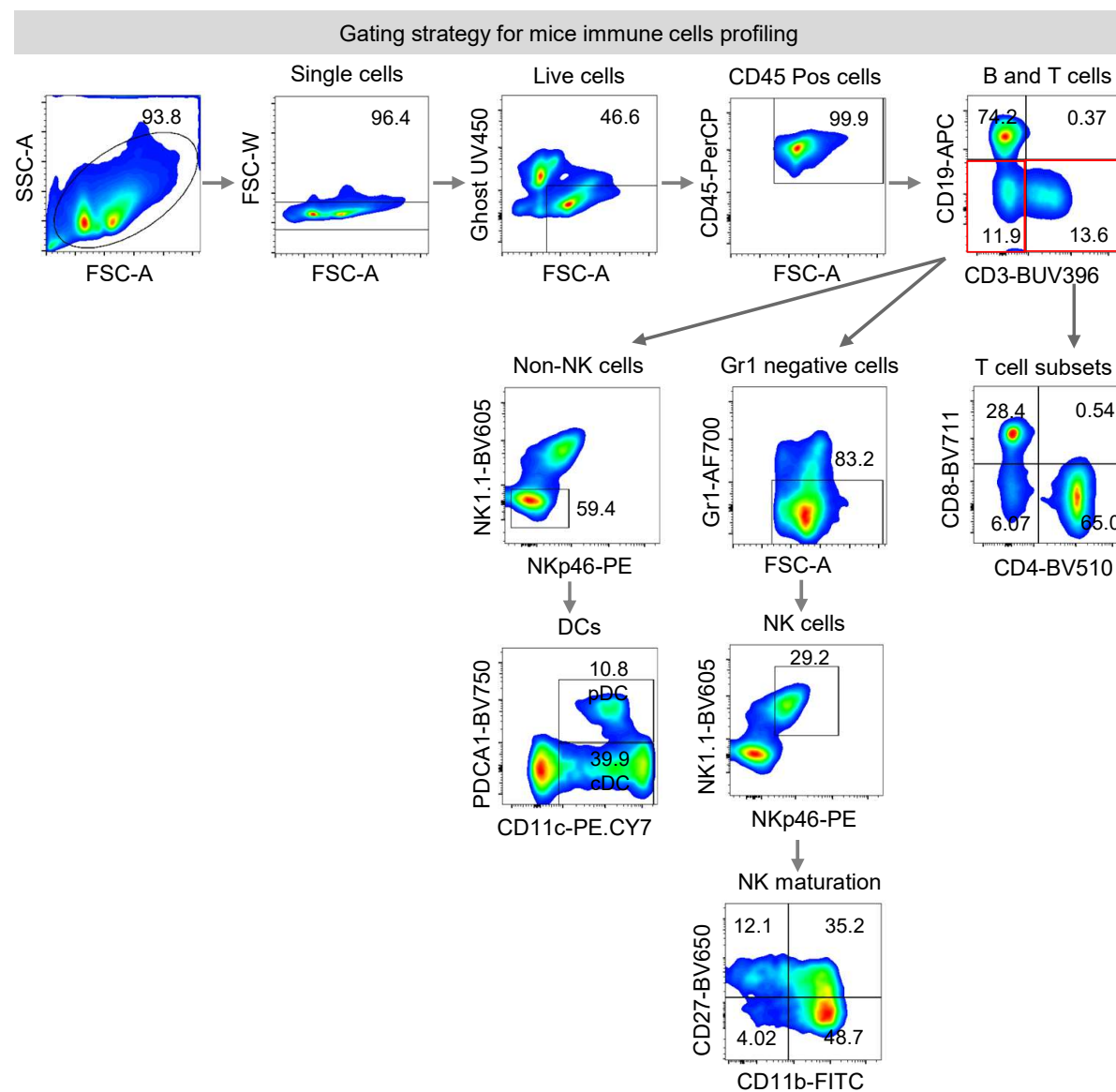
Figure S9: Gating strategy for flow cytometry analysis of mouse immune cells.

Figure S9: Gating strategy for flow cytometry analysis of mouse immune cells. From the lymphocytes cluster, singlets were gated followed by selection of live cells as Ghost-UV450⁻ and leucocytes as CD45⁺ cell fraction. T-cell subsets were analyzed from CD19⁺CD3⁺ cells. After the selection of non-B (non-leukemic) and non-T cells, NK cells were analyzed after gating on Gr1⁻ fraction. cDCs and pDCs were analyzed from the non-NK fraction.

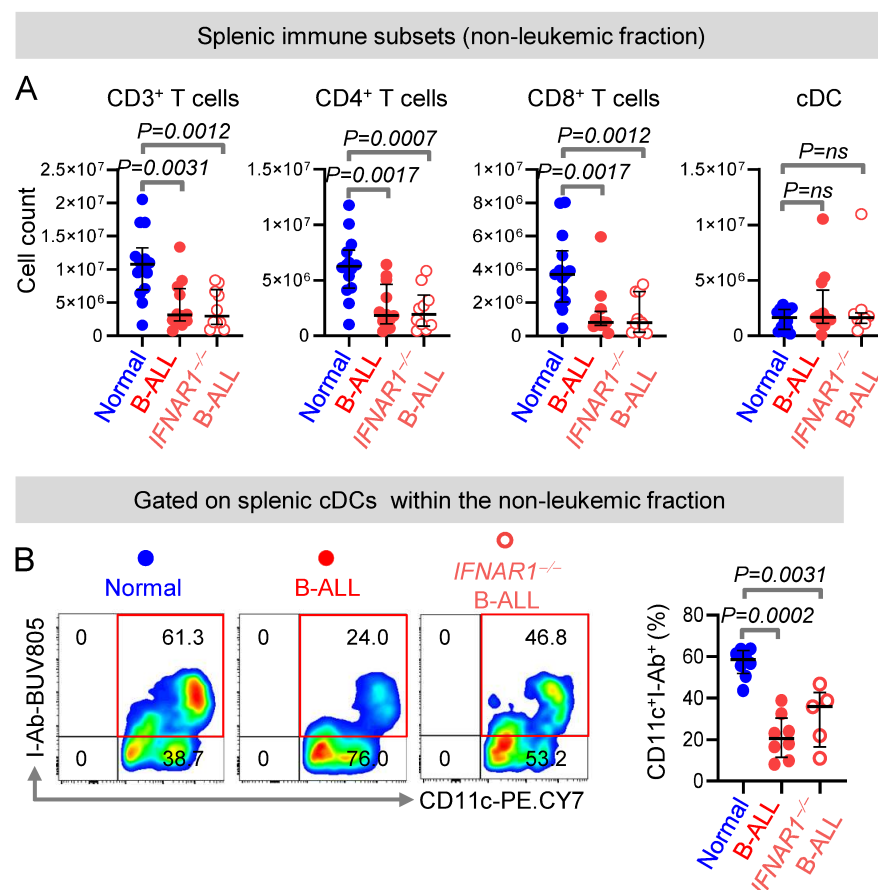
Figure S10: Ablation of *IFNAR1* does not exacerbate suppression of splenic T and DC subsets.

Figure S10: Ablation of *IFNAR1* does not exacerbate suppression of splenic T and DC subsets. (A) Comparison of pan T cells, T-cell subsets, and cDC counts in the non-leukemic fraction of the spleen of normal (n=14), *IFNAR1*^{+/+} *Eμ-Myc* B-ALL-bearing (n=12) and *IFNAR1*^{-/-} *Eμ-Myc* B-ALL-bearing (n=10;) mice. (B) Flow cytometry measurement of frequencies of I-Ab⁺ cells within pan DC (CD11c⁺) cells in the non-B, non-T, and non-NK cell fraction of the spleen of normal (n=8), *IFNAR1*^{+/+} *Eμ-Myc* B-ALL-bearing (n=8), and *IFNAR1*^{-/-} *Eμ-Myc* B-ALL-bearing (n=5) mice. P-values were calculated using Mann-Whitney U test. Exact p-values are provided whenever significant (<0.05) or trending to significance (0.05<p<0.1). ns = not significant.

Figure S11: Bone marrow T-cell subsets are reduced only upon by *IFNAR1* ablation during primary B-ALL development

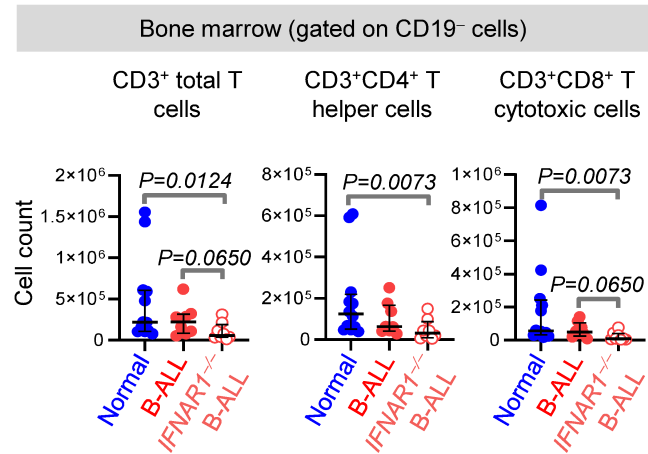


Figure S11: Bone marrow T-cell subsets are reduced only upon *IFNAR1* ablation during primary B-ALL development. Comparison of pan T cells and T-cell subsets in the non-leukemic fraction of the bone marrow of normal (n=12), *IFNAR1*^{+/+} *Eμ-Myc* B-ALL-bearing (n=8), and *IFNAR1*^{-/-} *Eμ-Myc* B-ALL-bearing (n=8) mice. Comparisons were conducted using Mann-Whitney U test. Exact p-values are provided whenever significant (<0.05) or trending to significance (0.05<p<0.1).

Figure S12: Purity of sorted mouse splenic NK cells used for NK adoptive transfer into ALL-bearing mice

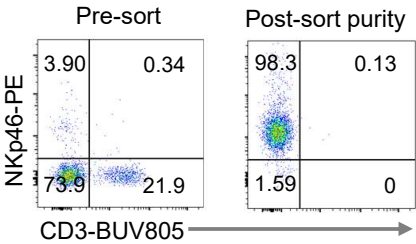


Figure S12: Purity of sorted mouse splenic NK cells used for NK adoptive transfer into ALL-bearing mice. Representative flow cytometry plots showing the pre-sort and post-sort purity of murine splenic NK cells isolated from normal syngeneic mice using magnetic-activated cell sorting.

Figure S13: IFN-Is drive NK surveillance and reduce progression of B-ALL

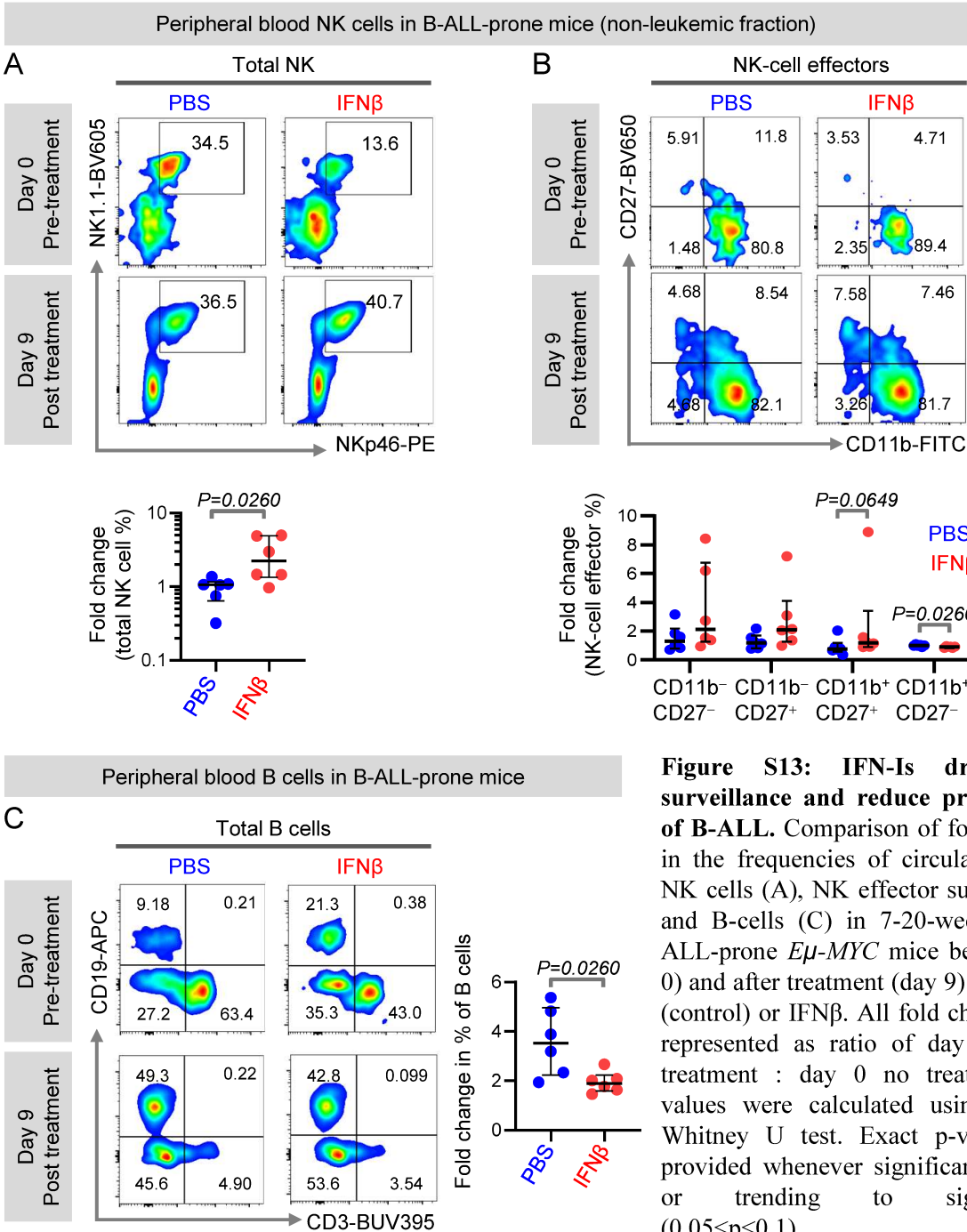


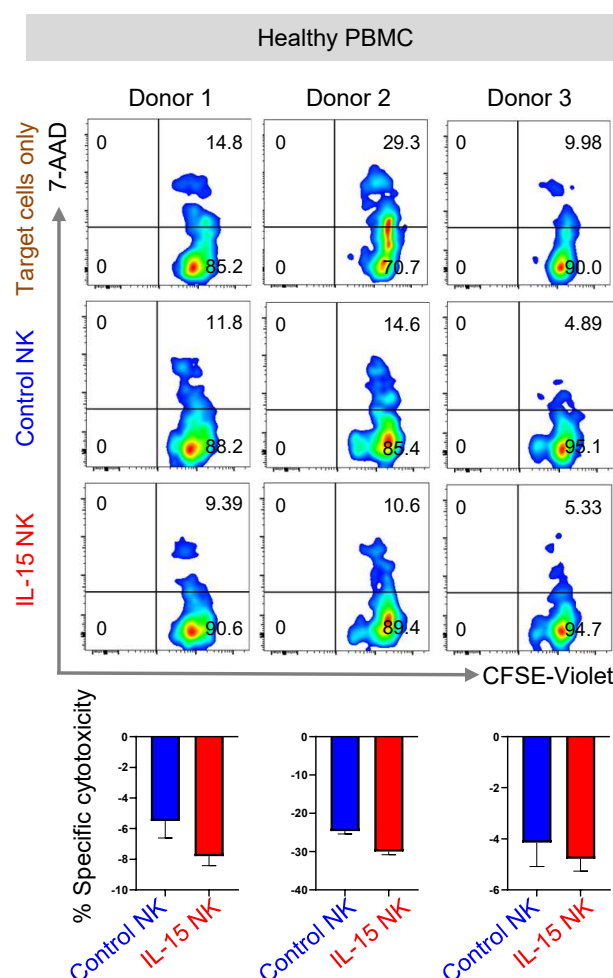
Figure S14: CRISPRa-engineered IL-15 NK cells are not toxic to healthy donor PBMC

Figure S14: CRISPRa-engineered IL-15 NK cells are not toxic to healthy donor PBMC. Flow cytometry to compare specific cytotoxicity of dCas9-VP64-GFP⁺ NK-92 cells transduced with control sgRNA-RFP (Control NK) or IL-15 sgRNA-RFP (IL-15 NK) against three independent healthy donor PBMC target cells. Effector: Target = 10:1. Comparisons were conducted using Student's t-test. Exact p-values are provided whenever significant (<0.05) or trending to significance (0.05<p<0.1).

Figure S15: *Inactivation of MYC restores autocrine IFN-I production and signaling in malignant human B cells*

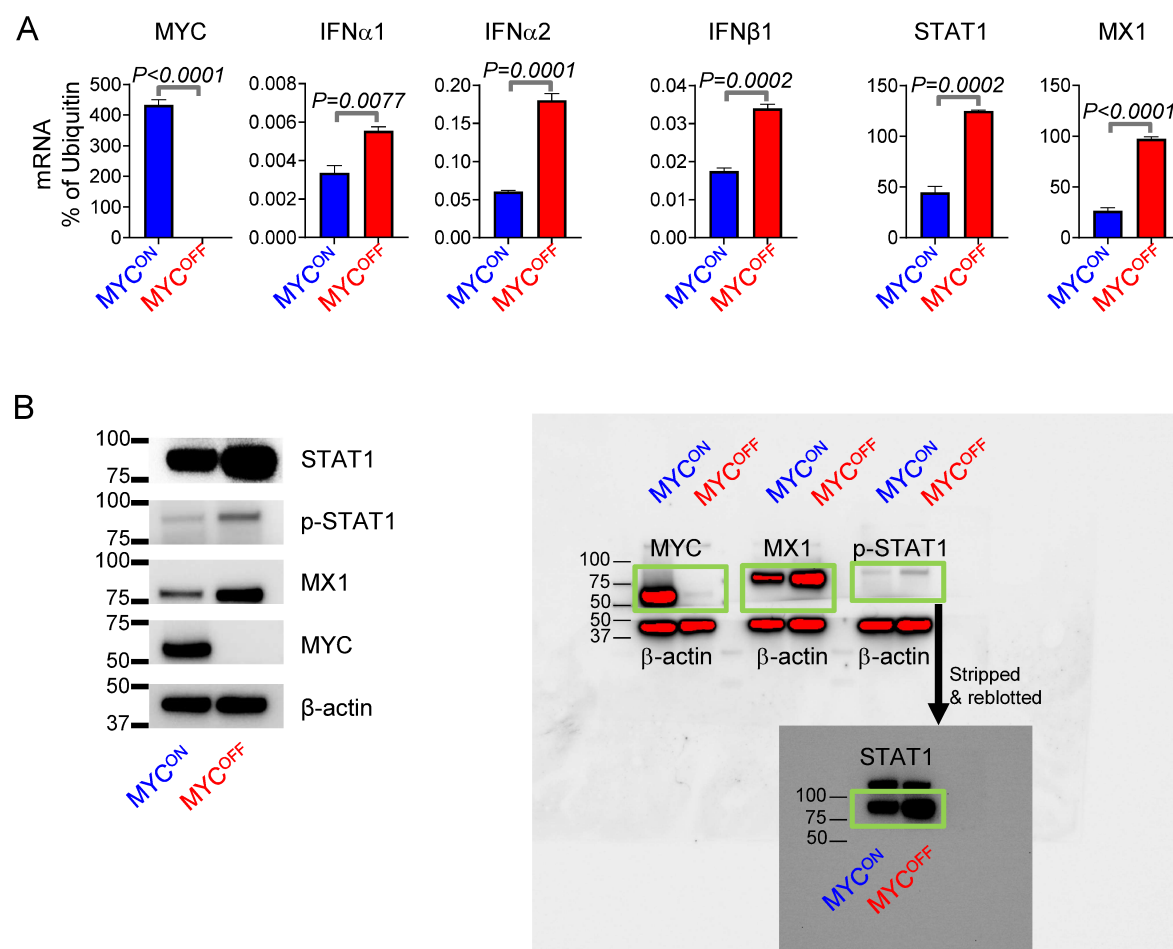


Figure S15: Inactivation of MYC restores autocrine IFN-I production and signaling in malignant human B cells. (A) Quantitation of expression of transcripts of MYC, IFN α 1, IFN α 2, IFN β 1, STAT1, and MX1 in MYC-overexpressing (MYC^{ON}) and MYC-inactivated (MYC^{OFF}) P493-6 malignant human B-cell line. Each qPCR sample was run in three technical replicates. The average of technical replicates is shown. P-values are calculated by unpaired t-test. Exact p-values are provided whenever significant (<0.05) or trending to significance (0.05<p<0.1). (B) Immunoblotting showing increase in global STAT1, p-STAT1, and MX1 after MYC inactivation in P493-6 cells (*left*). Full scan of blot (*right*).

Table S1: List of B-ALL patient samples used in the study

Patient ID	Age	Sex	Tissue Type	Cytogenetics	Translocation /Mutation status	Disease status	Source	Percentage of total IFN α 2b ⁺ cells
18067-HTB18-029	57	F	PBMC	Unknown	JAK2(G); JAK2(S) (Ph-like)	Diagnosis	City of Hope	0
18067-HTB19-1382	24	M	PBMC	Normal	EZH2; ETV6; KMT2D	Diagnosis	City of Hope	0
18067-LTB18-578	44	F	PBMC	Normal	KMT2D	Diagnosis	City of Hope	0.025
18067-HTB19-048	20	F	PBMC	47,XX,+22[6]	JAK2; JAK1 (Ph-like)	Diagnosis	City of Hope	0.055
18067-HTB19-937	41	F	PBMC	46,XX[16].ish t(X;14)(p22.33;q32.33)(5'IGH+;3'IGH+) [2]	IKZF1; JAK2(G); JAK2(S); PAX5 (Ph-like)	Diagnosis	City of Hope	0
18067-HTB19-376	30	F	PBMC	Unknown	KMT2D	Diagnosis	City of Hope	0.028
18067-HTB19-289	43	F	PBMC	47,XX,-2,t(3;15)(p23;q15), del(5)(q22q373),del(7)(p13p15), +del(9)(p21.2),der(9)del(9)(p13p22)del(9)(q22)x2, der(10)t(2;10)(q21;q26),del(12)(p11.2p13.3),add(17)(q25)x2,-20,+21,+mar[17]	KRAS; KMT2D; PAX5	Diagnosis	City of Hope	0.04
18067-LTB18-544	24	M	PBMC	47,XY,+X[6]	JAK2(G); JAK2(S) (Ph-like)	Diagnosis	City of Hope	0.014
18067-HTB19-1420	54	F	PBMC	46,XX,t(9;22)(q34.1;q11.2)[6];48,sl,+4,-16,+21,der(22)t(9;22) add(9)(q34.3),+der(22)t(9;22) add(9)[11] 47,sdl1,t(5;12)(q33;q13),-21[3]	KMT2C	Diagnosis	City of Hope	0.015

18067-HTB19-1424	25	Unknown	PBMC	46,XY,+X,der(1)dup(q42q12)?del(1)(q42q44),del(5)(q22q31),-7,t(8;9)(p21;q22),t(10;22)(p13;q13)[19]	KMT2D; NRAS; PAX 5	Diagnosis	City of Hope	0.012
65	33	F	Pheresis	47 - 48, xx, -4-11, +3-4 probable t(4;11)	t(4;11) KMT2A translocation	Diagnosis	University of Pennsylvania	
779	48	F	PBMC	46,XX,t(1;11)(p32;q23)[10]/48,idem,+X,+21[10]/FISH FOR MLL SPLIT POS 163/200 CELLS/FISH FOR BCR-ABL NEG 200 CELLS	t(1;11) KMT2A translocation	Diagnosis	University of Pennsylvania	
2142	30	M	Pheresis	46,XY,del(9)(p21p21)[6]/46,XY[24]	Ph-like	Diagnosis	University of Pennsylvania	
3113	44	F	PBMC	Unknown	KMT2A/AF1	Diagnosis	University of Pennsylvania	
4986	41	M	PBMC	46,XY[5]	Ph-like	Diagnosis	University of Pennsylvania	
4988	61	F	PBMC	46,XX,del(7)(p11.2)[7]/46,XX[13]	Ph-like	Refractory	University of Pennsylvania	
18067-HTB19-1191	40	F	BMMC	50,XX,-2,add(3)(q27.3),+6,i(6)(p10),-10,+12,del(12)(q24.1),t(14;18)(q32.33;q21.33),+der(14)t(14;18),+17,+2mar[20].ish der(2)t(2;8)(q37;q24.21)(3'MYC+)[2]	KMT2D; PTMA-MYC	Diagnosis	City of Hope	0.012
18067-HTB19-525	66	M	BMMC	35,X,-Y,-3,-7,-8,-9,-13,-14,-15,-16,-17,-22[11]; Sideline 1: 35,sl,add(18)(p11.2),del(20)(q13.1q13.3)[4];	MLL2; TP53	Diagnosis	City of Hope	0.02
18067-HTB19-1130	24	Unknown	BMMC	47,X,-Y,t(4;11)(q21;q23.3),+6,del(7)(p11.2),+i(7)(q10),?add(21)(p11.2)[14]	KMT2A	Diagnosis	City of Hope	0
18067-HTB19-054	21	F	BMMC	47,XX,+22[6]	Jak2; Jak1	Diagnosis	City of Hope	0.069
18067-HTB1-004	48	M	BMMC	47,XY,+X,del(6)(q21q25),der(7)t(7;8)(p13;q22),i(17)(q10),5~11dmin.ish t(Y;14)(p11.3;q32.33)(5'IGH+;3'IGH	TP53	Diagnosis	City of Hope	0.058

				+) [3] Sideline: 47,sl,del(10)(q22q26) [3] Nonclonal aberrations of Sideline: add(X)(p22.1), add(X)(q24), add(5)(p11.2), del(8)(q11.2), add(7)(p11.2), +10, add(17)(p11.2)				
18067-HTB22-0100	37	F	BMMC	46,XX,t(4;11;19)(q21;q23.3;q13.1) [13] Sideline 1: 46,sl,i(7)(q10) [4] Sideline 2: 47,sdl1,+21 [3] Nonclonal Aberrations of Stemline and Sidelines: t(1;3)(p36.1;p21), t(1;6)(p36.1;q23), t(1;18)(p13;q11.2), add(2)(p13), add(3)(p13), add(6)(q21)	KMT2A, TP53, WHSC1	Diagnosis	City of Hope	0.012
18067-HTB22-0386	39	F	BMMC	38,XX,-2,-3,-4,del(5)(q22q33),-7,del(7)(q22q26),der(8)del(8)(p21)del(8)(q11.2q21.2),add(9)(p13),der(10)t(10;?12)(q26;q13),-12,-13,-15,-16,?der(17)t(12;17)(p1?1.2;q?21),der(21)t(3;21)(p21;q22.3)[cp5]	EP300, MUTYH, PAX5, TP53	Diagnosis	City of Hope	0.38

Table S2: *Reagents and antibodies used for flow cytometry*

Name	Fluorophore	Clone	Dilution/ Concentration	Source
Anti-human CD45	FITC	2D1	1:100	Biolegend
Anti-human CD3	BUV805	UCHT1	1:100	BD
Anti-human CD19	BUV661	HIB19	1:100	BD
Anti-human CD14	BUV395	M5E2	1:100	BD
Anti-human CD56	BV510	NCAM16.2	1:100	BD
Anti-human CD16	BV711	3G8	1:100	BD
Anti-human HLA-DR	BUV737	G-46-6	1:100	BD
Anti-human CD11c	BV605	3.9	1:100	BD
Anti-human CD123	PE/Cy7	6H6	1:100	BD
Anti-human IFN- α 2b	APC	7N4-1	1:100	BD
Anti-human CXCR4	PECY5	12G5	1:100	Biolegend
Anti-pSTAT1 (pY701)	PE	4 α	10:100	BD
Anti-mouse CD45	PerCP	30-F11	1:100	Biolegend
Anti-mouse CD19	APC	1D3	1:100	BD
Anti-mouse CD3	BUV395	17A2	1:100	BD
Anti-mouse CD8	BV711	53-6.7	1:100	Biolegend
Anti-mouse CD4	BV510	RM4-5	1:100	Biolegend
Anti-mouse Gr1	Alexa Fluor 700	RB6-8C5	1:100	Biolegend
Anti-mouse NKp46	PE	29A1.4	1:100	BD
Anti-mouse NK1.1	BV605	PK136	1:100	Biolegend
Anti-mouse PDCA1	BV750	927	1:100	BD
Anti-mouse CD11c	PC/CY7	N418	1:100	Biolegend
Anti-mouse CD27	BV650	LG.3A10	1:100	Biolegend
Anti-mouse CD11b	FITC	M1/70	1:100	Biolegend
Anti-mouse I-Ab	BUV805	25-9-17	1:100	BD
Ghost-Dye UV450	NA	NA	1:100	Tonbo Biosciences
CSFE-Violet	NA	NA	2.5 μ M	ThermoFisher Scientific
Perm Buffer IV 10X	NA	NA	0.5X	BD
BD Cytofix/Cytoperm fixation and permeabilization solution	NA	NA	1X	BD
7AAD	NA	NA	1:100	Biolegend
Fc block	NA	NA	1:100	BD
eBioscience™ Protein Transport Inhibitor Cocktail (500X)	NA	NA	1X	ThermoFisher SCIENTIFIC
ODN2395	NA	NA	3 μ M	InvivoGen

Table S3: *Reagents and antibodies used for mass cytometry*

Metal label	Target	Clone	Source	Concentration (µg/mL)	Titre (µg/mL)
141Pr	HLA-DR	L243	Custom, Biolegend	425	2
145Nd	CD4	RPA-T4	Fluidigm	500	5
146Nd	CD8	RPA-T8	Fluidigm	500	5
147Sm	CD20	2H7	Fluidigm	500	5
153Eu	CD45RA	HI100	Fluidigm	500	5
154Sm	CD3	UCHT1	Fluidigm	500	5
158Gd	CD33	WM53	Fluidigm	500	5
160Gd	CD14	M5E2	Fluidigm	500	5
166Er	IL-2	MQ1-17h12	Fluidigm	500	5
167Er	CD27	L128	Fluidigm	500	5
176Yb	CD56	NCAM16.2	Fluidigm	500	5
209Bi	CD16	3G8	Fluidigm	500	5

Table S4: *Primers used for qPCR analysis*

Name	Forward	Reverse
IFN α R1	CGAGGCCGAAGTGGTTAAAAG	ACGGATCAACCTCATTCCAC
IFN α R2	ACCGTCTGCTTTTGATGGGT	AGAGGGTGTAGTTAGCGGGT
IFN β 1	GCCTTTGCCATCCAAGAGATGC	ACACTGTCTGCTGGTGGAGTT
IFN α 1	GGATGTGACCTTCCTCAGACTC	ACCTTCTCCTGCGGGAATCCAA
IFN α 2	ATCCAGAAGGCTCAAGCCATCC	GGAGGGTTGTATTCCAAGCAGC
STAT1	TGGTGAAATTGCAAGAGCTG	CAGACTTCCGTTGGTGGATT
MX1	CTCTGGGTGTGGAGCAGGAC	GAGGGCCACTCCAGACAGTG
IL-15	GTAGGTCTCCCTAAAACAGAGGC	TCCAGGAGAAAGCAGTTCATTGC
OAS1	GAGGTGGAGTTTGATGTGCTGC	GTGAAGCAGGTAGAGAACTCGC
Ubiquitin	AGCCCAGTGTTACCACCAAG	ACCCAAGAACAAGCACAAGG
IL-15 (Human)	AACAGAAGCCAAGTGGGTGAATG	CTCCAAGAGAAAGCACTTCATTGC
MYC (Human)	CTGCGACGAGGAGGAGAACT	GGCAGCAGCTCGAATTTCTT
IFN α 1 (Human)	TTGACTCATACACCAGGTCACG	AGCATGGTCATAGTTATAGCAGGG
IFN α 2 (Human)	TGGGCTGTGATCTGCCTCAAAC	CAGCCTTTTGGAAGTGGTTGCC
IFN β 1 (Human)	CTTGGAATCCTACAAAGAAGCAGC	TCCTCCTTCTGGAAGTGTGCA
STAT1 (Human)	CCGTTTTTCATGACCTCCTGT	TGAATATTCCCCGACTGAGC
MX1 (Human)	GGCTGTTTACCAGACTCCGACA	CACAAAGCCTGGCAGCTCTCTA
Ubiquitin (Human)	GCCGCACTCTTCTGACTACAAC	ACCTCCAGAGTGATGGTCTTGC

Table S5: *Antibodies used for immunoblotting*

Name	Clone ID/ Catalog No	Specificity	Dilution/ Concentration	Source
Anti- β -Actin	8H10D10	Mouse/Human	1:1000	Cell Signaling Technology
Anti-cMYC	D84C12	Mouse/Human	1:500	Cell Signaling Technology
Anti-phospho STAT1 (Ser727)	#9177S	Mouse/Human	1:500	Cell Signaling Technology
Anti-STAT1	#9172S	Mouse/Human	1:1000	Cell Signaling Technology
Anti-MX1	D3W71	Mouse/Human	1:1000	Cell Signaling Technology

